UNIVERSITÄTSKLINIKUM HAMBURG-EPPENDORF

Zentrum für Experimentelle Medizin, Institut für Tumorbiologie

Direktor: Prof. Dr. med. Klaus Pantel

The effects of electromagnetic fields on breast cancer cell lines AND exosomal microRNAs in blood of breast cancer patients

Dissertation

zur Erlangung des Grades eines Doktors der Medizin /Zahnmedizin
an der Medizinischen Fakultät der Universität Hamburg.
.

vorgelegt von:

Qingtao Ni
aus Jiangsu (China)

Hamburg 2018

(wird von der Medizinischen Fakultät ausgefüllt)

Angenommen von der
Medizinischen Fakultät der Universität Hamburg am: 4.10.2018

Veröffentlicht mit Genehmigung der
Medizinischen Fakultät der Universität Hamburg.

Prüfungsausschuss, der/die Vorsitzende: H. Schwetzschbach

Prüfungsausschuss, zweite/r Gutachter/in:

Contents

1. Introduction 1
1.1. Breast cancer 1
1.1.1. Metastasis of BC....1
1.1.2. Symptom and diagnosis of BC....2
1.1.3. Risk factors of BC....3
1.1.4. Treatment and prognosis of BC....3
1.1.5. Subtypes of BC....4
1.1.6. Classifications of BC....5
1.2. Ductal Carcinoma in Situ....7
1.3. Electromagnetic field....8
1.3.1. Function of EMF....10
1.4. DNA methylation....10
1.5. DNA hydroxymethylation....12
1.6. Exosomes....12
1.6.1. Exosome biogenesis....12
1.6.2. Exosomes function....14
1.7. MicroRNAs....14
1.7.1. MicroRNAs biosynthesis....14
1.7.2. Characteristics of miRNAs....16
2. Material and Methods....17
2.1. Cell lines....17
2.2. Depletion exosomes from FCS....17
2.3. EMF exposure experiments....18
2.4. Counting of cells....19
2.5. DNA isolation from cell lines....20
2.6. Detection of DNA methylation and DNA hydroxymethylation....20
2.6.1. Detection of DNA methylation....20
2.6.2. Detection of DNA hydroxymethylation....21
2.7. Isolation of exosomes from cell culture supernatant....22
2.8. Detection of exosome protein....23
2.9. Quantification of exosomes by ELISA....23
2.10. Study populations and plasma samples....24
2.11. Verification of hemolysis in plasma samples....25
2.12. Extraction of exosomes from plasma....26
2.13. Western blot....27
2.13.1. SDS polyacrylamide gel electrophoresis....27

2.13.2. Transfer 27
2.13.3. Blocking 28
2.13.4. Protein detection 29
2.14. Extraction of miRNAs from exosomes 30
2.15. Conversion of exosomal miRNAs into cDNA 30
2.16. Preamplification of cDNA 31
2.17. PCR-based TaqMan miRNA arrays 32
2.18. Single TaqMan PCR analyses of miR-16, miR-30b and miR-93 34
2.19. Data normalization and statistical analyses 35
3. Results 37
3.1. Investigations of the effects of EMFs on BC cell lines 37
3.1.1. Work flow 37
3.1.2. The impact of EMF exposure on cell number 38
3.1.3. The impact of EMF exposure on 5-mC DNA 38
3.1.4. The impact of EMF exposure on 5-hmC DNA 39
3.1.5. The impact of EMF exposure on the levels of exosomes in cell lines 40
3.1.6. Repetition of experiments II and VIII 41
3.2. Circulating exosomal microRNAs in blood of BC patients 43
3.2.1. Work flow 43
3.2.2. Verification of exosomes 44
3.2.3. MiRNA profiling in exosomes of BC and DCIS patients 45
3.2.4. Association of exosomal miR-16, miR-30b and miR-93 with the clinicopathological parameters of BC patients 50
4. Discussion 52
4.1. Investigations of the effects by EMFs on BC cell lines 52
4.2. Circulating exosomal microRNAs in blood of BC patients 53
5. Summary 56
6. List of abbreviations 58
7. Reference 61
8. Acknowledgement 72
9. Curriculum Vitae 73
10. Eidesstattliche Versicherung 75

1. Introduction

1.1. Breast cancer

Breast cancer (BC, Figure 1.1) ranks at fifth position in all cancer types, and is the second leading cause of cancer death in women, just after lung cancer (1). It occurs not only in women, but also in men. Regarding the American Cancer Society's estimates in the United States, around 266,120 new diagnoses of BC are expected in women for 2018, and around 40,920 women are likely to die from this disease (2).

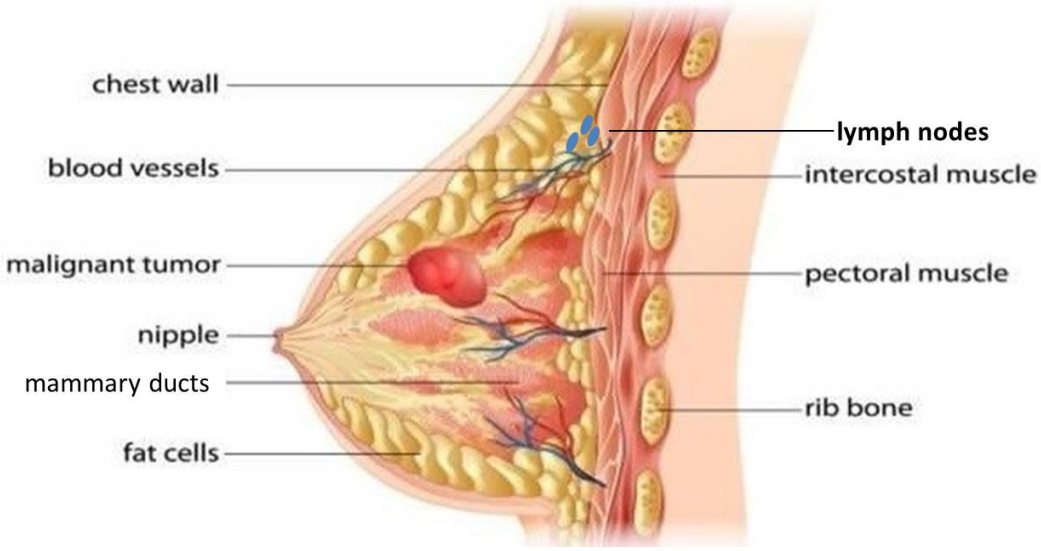

Figure 1.1. Anatomy of BC (modified from Blue Ring Media / Shutterstock)

BC develops when breast cells uncontrolledly divide and invade into neighboring tissues, such as lymph nodes, nipple, chest wall, rib bone, muscles and mammary ducts, or spread (metastasize) to different parts of the body by lymph nodes and blood vessels.

1.1.1. Metastasis of BC

Metastasis comprises a cascade of tumor spread starting with local invasion of the surrounding tissue, spreading into the blood or lymphatic vessels and ending with dissemination of tumor cells to distal organs (Figure 1.2) (3). Locoregional spread of BC occurs mainly through the lymph nodes, with the most common site being sentinel lymph

node. Cancer cells also can invade nearby healthy tissues directly, such as skin, rib bone and pectoral muscle. If cancer cells block the mammary ducts, there will be nipple retraction or elevation.

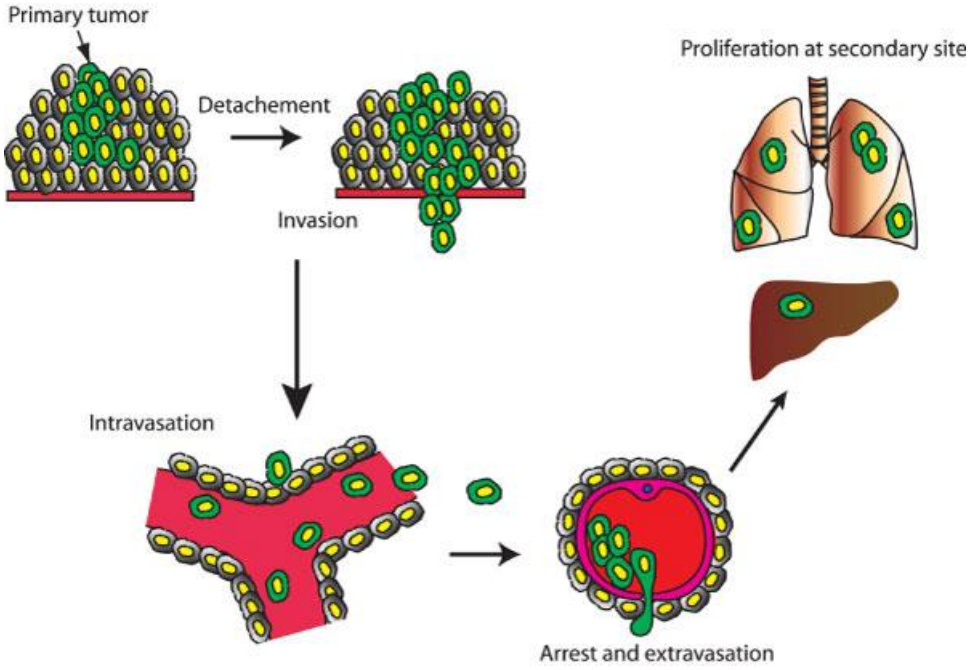

Figure 1.2. The metastatic process (from Hunter et al., Breast Cancer Res, 2008)

The initial steps of metastasis include proliferation of the primary tumor and invasion through adjacent tissues and basement membranes. Individual tumor cells undergo epithelial-mesenchymal transition (EMT) and detach from the primary tumor mass. They invade blood vessels or lymphatic channels, and are carried to a distant organ. Subsequently, tumor cells arrest in small vessels within the distant organ, extravade into the surrounding tissue, undergo mesenchymal-epithelial transition (MET), and proliferate at the secondary site.

1.1.2. Symptom and diagnosis of BC

Early stage BC often does not have typical symptoms and signs, therefore, it is not usually be easily detected. The most common symptom of BC is a new lump or mass. Other symptoms of BC include skin depressions, nipple retraction and spontaneous removal from the nipple or bloody discharge (4). BC is often found through physical examination or mammograms. Breast ultrasound, magnetic resonance imaging (MRI) and breast biopsy are

usually used as diagnostic tools. Some different biomarkers, such as hormone receptor, human epidermal growth factor 2 (HER2) and carcinoembryonic antigen(CEA) status are used to identify BC subtypes (5).

1.1.3. Risk factors of BC

The incidence of BC is related to a variety of risk factors, such as age, family history, genetics and epigenetics. The incidence rate of BC is much higher in women at age of 30 than 20 (6). About two thirds of invasive BCs are found in women aged over 55 years. Women who have close relatives with BC have a higher risk to contract BC (7). The most common cause of hereditary BC is an inherited mutation in BRCA1 (breast cancer, early onset 1) and BRCA2 (breast cancer, early onset 2). In normal cells, these genes code proteins which can repair damaged DNA. Mutated versions of these genes can lead to abnormal cell growth, resulting in carcinogenesis. It is reported that mutated BRCA1 and BRCA2 gene increase the risk of developing BC more than 4-fold (8). Further risk factors are insulin and adiponectin levels (9) mammographic breast density (10), radiation exposure, postmenopausal obesity, lack of exercise, alcohol consumption and hormone replacement therapy. Some social problems, such as younger age at menarche, older age at first pregnancy, no pregnancy, shorter or no breastfeeding time, and a later menopause also support BC development (11).

1.1.4. Treatment and prognosis of BC

The treatments of BC generally depend on the subtype and stage. Local treatments of BC are surgery and radiation therapy. To reduce the risk of recurrence, hormonal therapy and chemotherapy may be used. In the last years, targeted biologic therapies have been increasingly applied. For example, the combination of trastuzumab with chemotherapy has led to significant reduction in BC recurrence and mortality in HER2-positive BC (12). The early-stage screening reduces mortality of BC drastically (13, 14). For example, BC patients diagnosed at stage I have a higher 5-year survival rate of 88 %, whereas the 5-year survival rate of stage IV BC is only 15 % (15). The 10-year incidence of locoregional recurrence

historically in early stage BC has been 3 % to 8 % after mastectomy and about 10 % to 12 % after breast-conserving therapy (16).

1.1.5. Subtypes of BC

Human breast tumors are heterogeneous. They are primarily defined by hormone receptor status (ER, PR) and HER2 as well as the proliferation marker Ki-67 into four molecular subtypes (17). These four molecular subtypes are commonly recognized as luminal A, luminal B, HER2-positive, and triple-negative BC (Table 1.1).

Table 1.1. Subtypes of BC (modified from Dai et al., American Journal Cancer Research, 2015)

Intrinsic subtype	growth receptor status	Grade	Outcome	Prevalence
Luminal A	ER+ and/or PR+, HER2-, Ki67-	1|2	good	24 %
Luminal B	ER+ and/or PR+, HER2-, Ki67+	2|3	intermediate	39 %
	ER+ and/or PR+, HER2+, Ki67+		poor	14 %
HER2-positive	ER-, PR- and HER2+	2|3	poor	11 %
Triple-negative	ER-, PR- and HER2-	3	poor	12 %

Luminal A BC is hormone receptor positive, is low-grade and has the best prognosis. Luminal B BC is of higher grade and a significantly worse prognosis than the luminal A subtype. It is the most common type of all BC. They can be treated by endocrine therapy alone or a combination with chemotherapy. HER2-positive BC patients have the second poorest outcome. The highly poor survival of triple-negative BC patients is caused by the lack of effective and specific therapy (18). Since HER2-positive and triple-negative BC patients do not express any hormone receptor, an endocrine therapy is not efficient. However, HER2-positive BC can be treated by trastuzumab which binds to this receptor and blocks the ability of the cancer cells to receive growth signals (19).

1.1.6. Classifications of BC

1.1.6.1. Stage of BC

BC is staged according to the size of the primary tumor and lymphatic or distant metastasis. There are different ways of staging BC. The most common staging is from stage 0 to 4, which are grouped in substages (Table 1.2).

Table 1.2. Tumor stages of BC (from Atoum et al., Indian Journal of Cancer, 2010)

Stage	Definition
Stage 0	Tumors that have not grown beyond their site of origin and invaded the neighboring tissue.
Stage 1	Tumor size <2 cm, no metastases to other organs and tissues.
Stage 2a	Tumor <2 cm in cross-section with the involvement of the lymph node or tumor from 2 to 5 cm without the involvement of the axillary nodes.
Stage 2b	Tumor more than 5 cm in cross-section (the result of axillary lymph node research is negative for cancer cells) or tumor from 2 to 5 cm in diameter with the involvement of axillary lymph nodes.
Stage 3a	Local spread of BC, tumor more than 5 cm with spread to axillary lymph nodes or tumor of any size with metastases in axillary lymph nodes, which are knitted to each other or with the surrounding tissues.
Stage 3b	Tumor of any size with metastases into the skin, chest wall or lymph nodes of the mammary gland (located below the breast inside of the chest).
Stage 3c	Tumor of any size with a more widespread metastases and involvement of more lymph nodes.
Stage 4	Tumors spread to parts of the body that are located far removed from the chest (bones, lungs, liver, brain or distant lymph nodes).

The staging was defined by the NCI-NIH (National Cancer Institute-National Institute of Health), USA, and revised by the American Joint Committee on Cancer (AJCC).

1.1.6.2. Grading of BC

The grade of BC reflects the differentiation grade of cancer cells. The most common grading system is the Scarff-Bloom-Richardson (SBR) histological tumor grading (Table 1.3). This grading system includes tubule formation, nuclear pleomorphism and mitoses. The score varies from 3 to 9 and is summarized as one of the three histological grades (20).

Table 1.3. SBR histological tumor grading of BC (from Bansal et al., Journal of Cancer Research and Therapeutics, 2014)

Feature	Score
Tubule formation (%)	
Majority of tumor (>75)	1
Moderate degree (10-75)	2
Little or none (<10)	3
Nuclear pleomorphism	
Small, uniform cells	1
Moderate increase in size/variation	2
Marked variation	3
Mitotic counts (per 10-40× fields)	
0-5 (histology) or 0-1(cytology)	1
6-10 (histology) or 2-4 (cytology)	2
>11 (histology) or >5(cytology)	3
Grade 1 (well differentiated)	3-5
Grade 2 (moderately differentiated)	6-7
Grade 3 (poorly differentiated)	8-9

SBD=Scarff-Bloom-Richardson

1.1.6.3. Histology of BC

BC is heterogeneous with many different subtypes, such as non-special type (NST), lobular, tubular, mucinous, medullary, papillary and micropapillary. Among them, mucinous, medullary, papillary and micropapillary BCs are extremely rare. Lobular BC is the most common morphological subtype of all BC, comprising up to 15 % of all cases (21). Tubular

carcinoma normally occurs in younger age women, it accounts for about 5 % of all BC and has a good prognosis (Figure 1.3) (22).

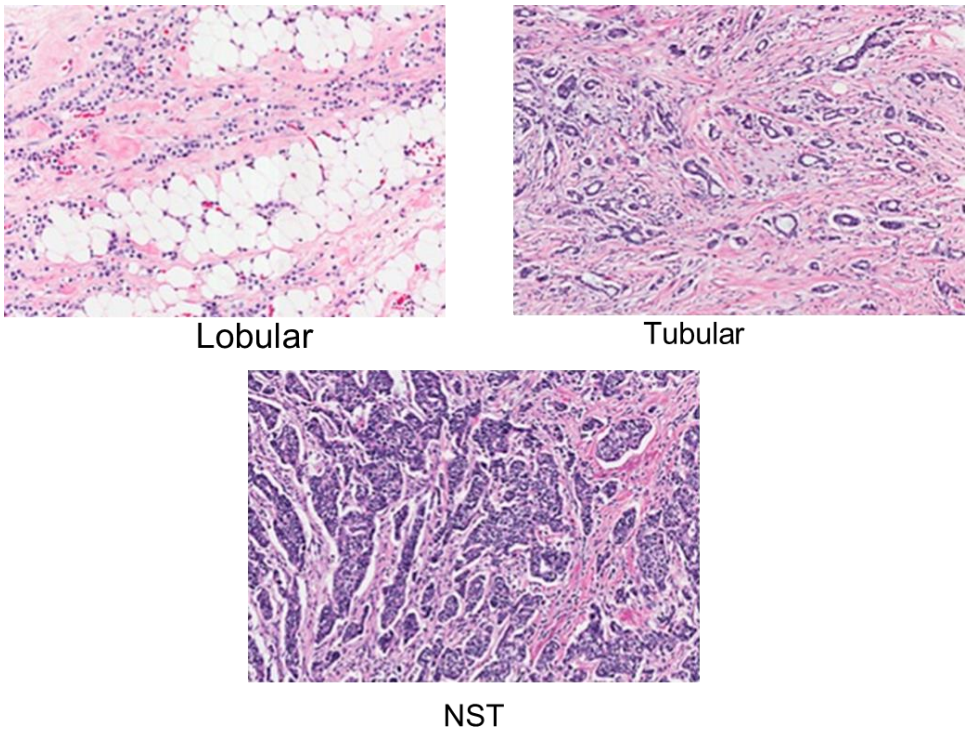

Figure 1.3. Main BC histological types (from Rebecca Mayrhofer et al., Magn Reson Insights, 2013)

Haematoxylin and eosin (H&E) staining of the cells and 40× enhancement microscopy. Lobular carcinoma: The tumor shows uniform tumor cells mostly arranged in a single file. Some of the tumor cells show intracytoplasmic luminae. Tubular carcinoma: The tumor is highlighted by irregularly distributed rounded and angulated tubules with open luminae. The tubules are lined by a single layer of epithelial cells and surrounded by desmoplastic stroma. Non-special histological type (NST): The tumor is arranged in cords, clusters and trabeculae with scanty tubule formation and several mitoses per high-power image field.

1.2. Ductal Carcinoma in Situ

Ductal carcinoma in situ (DCIS) is a non-invasive BC type which arises within terminal duct lobular units (23). It is also considered to be an established morphologic precursor of invasive breast carcinoma (24, 25). According to the American Cancer Society, about 60,000

cases of DCIS are diagnosed in the United States each year. The increased incidence of DCIS is due to the mammography over the past 30 years (26, 27). Every year, 80 % of DCIS cases are detected by mammography (28). DCIS generally has no signs or symptoms (29). Some patients may have a lump in the breast, blood, serosanguinous, serous or clear liquids come out of the nipple (30). In most cases, DCIS patients are treated by breast-conserving surgery or mastectomy. Traditionally treatments for DCIS include radiation and endocrine therapy (31). DCIS is often curable, but 15 % DCIS patients can also develop an invasive BC in 10 years (23, 32, 33). The detection of levels of HER2 and Ki-67 in DCIS patients may help predict for both overall survival and invasive recurrence (34).

1.3. Electromagnetic field

The electromagnetic field (EMF), a combination of an electric field and a magnetic field, is a physical field produced by the movement of electrically charged objects (Figure 1.4) (35). EMF is a smooth, continuous field, propagated in a wavelike manner, as described by the Maxwell equation. It has different wavelengths, frequencies and energies. In daily life, microwave, visible light and X-rays in medicine are EMFs. The energy of the radiation is proportional to the frequency, so that X-rays and gamma rays with high frequencies are harmful to the health (Figure 1.5). The cell information therapy (CIT) uses EMF with frequencies from 3 Hz to approximate 100 Hz. These frequencies belong to the low-frequency range of the spectrum, meaning that the energy used in the CIT is much lower than conventional radiation therapies and even lower than the radiant power of an ordinary smartphone (36).

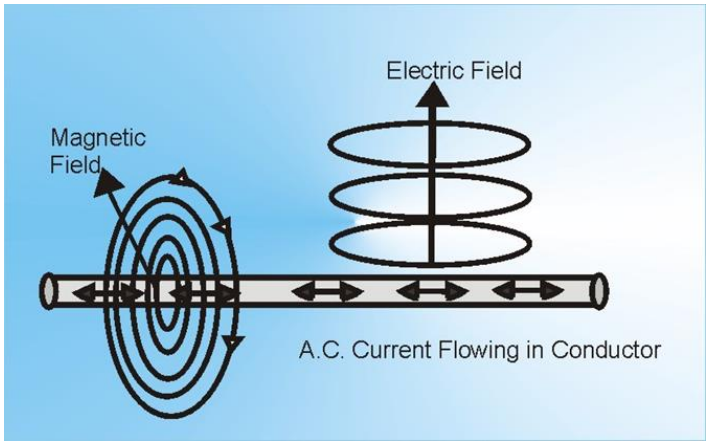

Figure 1.4. Schematic diagram of EMF (from EMsafety website)

EMF is a physical field produced by the movement of electrically charged objects. Stationary charges produce the electric field, whereas alternating current (A.C.) flowing in the conductor produces the magnetic field. This results in a combination of an electric field and a magnetic field.

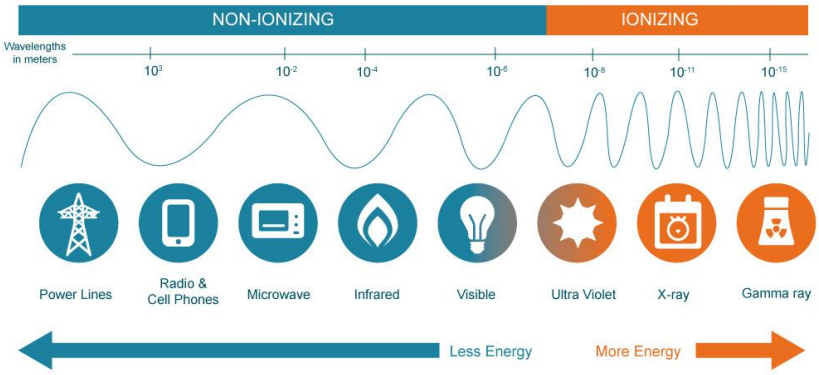

Figure 1.5. EMF exists everywhere in daily life (from Quora website)

The shorter the wavelength of EMFs, the stronger the energy. Ultra violet, X-rays and gamma rays are ionizing radiation. They have the potential to cause cellular and DNA damage. Non Ionizing EMFs are generally considered harmless to humans, such as extremely low frequency (ELF), radiofrequency, microwaves, infrared radiation and visible light.

1.3.1. Function of EMF

EMF was detected for more than 20 years. In 1993, Bassett found that EMF has effects on nerve regeneration, wound healing, graft behavior, diabetes, myocardial and cerebral ischemia, and even on malignant diseases (37). In 1994, the first device for CIT was successfully applied in the treatment of respiratory diseases, inflammatory processes, cartilage damage and wound healing. A specific EMF exposure can change cellular processes (38), e.g., affecting the Mitogen-activated protein (MAP) kinase pathway resulting in growth inhibition of malignant cells (39). Zhang et al. showed that calcium uptake in osteoblasts increased after exposure with EMF, in the range of 50 Hz and 0.8 mT (40). EMF decreased the cell viability of the pineal gland in a specific time (41). It also promoted bone fracture healing and reduced knee pain (42, 43). A 50 Hz intensity field could change the mRNA levels of antioxidant genes at condition of a 15 min field-on and a 15 min field-off (44). Crocetti et al. found that EMF had an effect on BC without affecting normal tissues (45). Although, it is critical to find the appropriate strength of EMF to treat diseases (46), its application in cancer treatment may be promising.

1.4. DNA methylation

Changes in DNA methylation are a common early event in carcinogenesis (47). In mammals, cytosine, at the 5th carbon atom position, is methylated within a cytosine-phosphate-guanine (CpG) dinucleotides by DNA methyltransferases (DNMT) resulting in a 5 methylcytosine (5-mC, Figure 1.6.a) (48, 49). Within the DNMT family, Dnmt1 is mainly involved in maintaining DNA methylation during DNA replication (Figure 1.6.b) (50). DNA methylation is essential for the differentiation and maturation of the mammalian central nervous system (51) and among others, for stem cell differentiation, X chromosome inactivation and transposition factor inhibition (52). DNA methylation usually refers to promoter inactivation, leading to repression of gene expression. In cancer cells, the genome is usually hypomethylated (53), but the

regions of tumor suppressor genes are usually hypermethylated, thus inactivated (Figure 1.7).

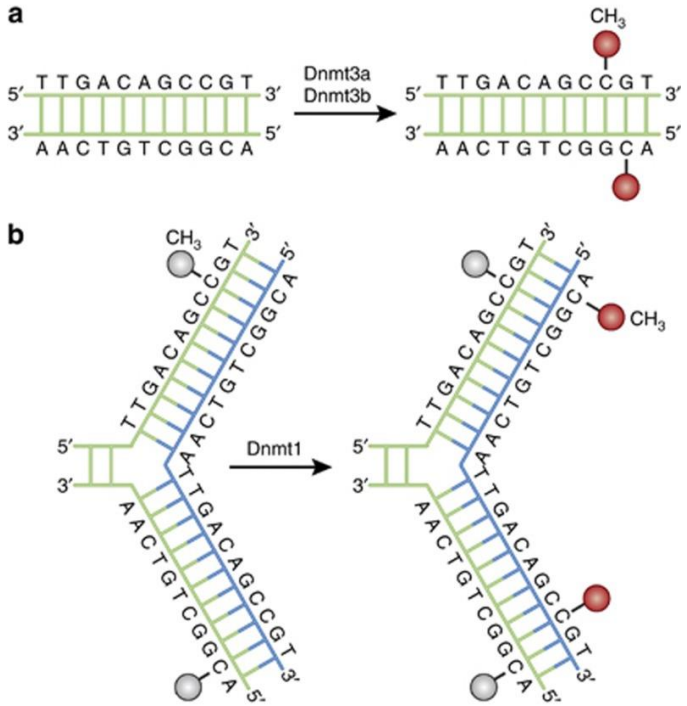

Figure 1.6. DNA methylation pathways (from Lisa, Neuropsychopharmacology, 2013)

(a) Dnmt3a and Dnmt3b establish the first DNA methylation pattern. (b) Dnmt1 maintains this pattern during replication. When DNA undergoes semi-conservative replication, the parental DNA strand retains the original DNA methylation pattern (gray). Dnmt1 associates at the replication foci and precisely copies the DNA methylation pattern of the parental DNA strand by adding methyl groups (red) to cytosine within CpG dinucleotides of the newly replicated daughter strand (blue).

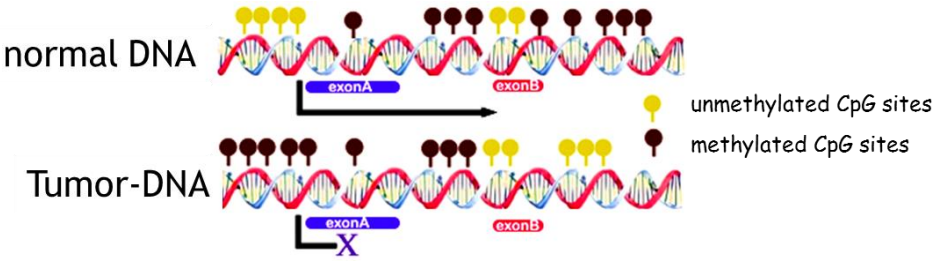

Figure 1.7. Comparison of DNA methylation pattern between normal and tumor DNA (from Arvind Shukla, Journal for Advanced Research in Applied Sciences, 2016)

Tumor DNA is usually hypomethylated, but regions of tumor suppressor genes are usually hypermethylated. Demethylated regions in normal DNA are methylated in tumor DNA and conversely methylated regions in normal DNA are demethylated in tumor DNA.

1.5. DNA hydroxymethylation

In 2009, 5-hydroxymethylcytosine (5-hmC) was detected for the first time in mouse Purkinje neurons and embryonic stem cells (54, 55). DNA hydroxymethylation refers promoter activation, leading to gene expression. 5-hmC is generated by hydroxylation of 5-mC by the Ten-eleven translocation proteins (TET1, 2, 3) family of cytidine oxygenase enzymes (Figure 1.8) (56). In human, the abundance of 5-hmC is different in each organs. For example, the brain tissue with 0.67 % has the highest level, whereas the placenta with 0.06 % and breast tissue with 0.05 % display the lowest levels of 5-hmC (57).

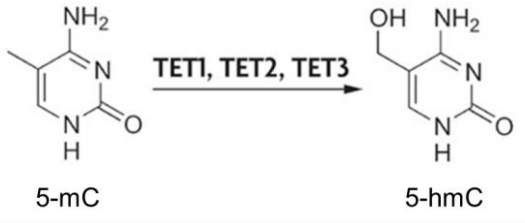

Figure 1.8. Scheme on the hydroxymethylation of 5-mC to 5-hmC (modified from Maria A Hahn et al., Genomics, 2014)

5-mC is converted to 5-hmC by the TET family of cytidine oxygenase enzymes.

1.6. Exosomes

1.6.1. Exosome biogenesis

In 1983, Harding et al. and Pan et al. detected exosomes for the first time (58, 59). Exosomes are small-membrane vesicles with a diameter of 30-100 nm, and contain proteins, nucleic acids (DNAs, RNAs, microRNAs) and lipids (60, 61). The composition of exosome cargos depends on cell types and different cellular conditions or treatments (62). The

database ExoCarta summarizes the different exosomal cargos (63). Exosomes can be released by many different cell types, such as immune cells, mesenchymal cells and cancer cells (64).

Exosomes are initially produced by endocytosis. The inward budding of membranous vesicles of endosomes form multivesicular bodies (MVBs) carrying genetic material and proteins (65). Late MVBs are integrated into lysosomes where they are degraded, or fuse with the cell membrane. Then, they are released into the extracellular space as exosomes. The extracellular exosomes bind to specific ligands on the surface of a recipient cell and discharge their cargos in to the cell (Figure 1.9) (66). The released nucleic acids may then be functionally active in the recipient cell (67).

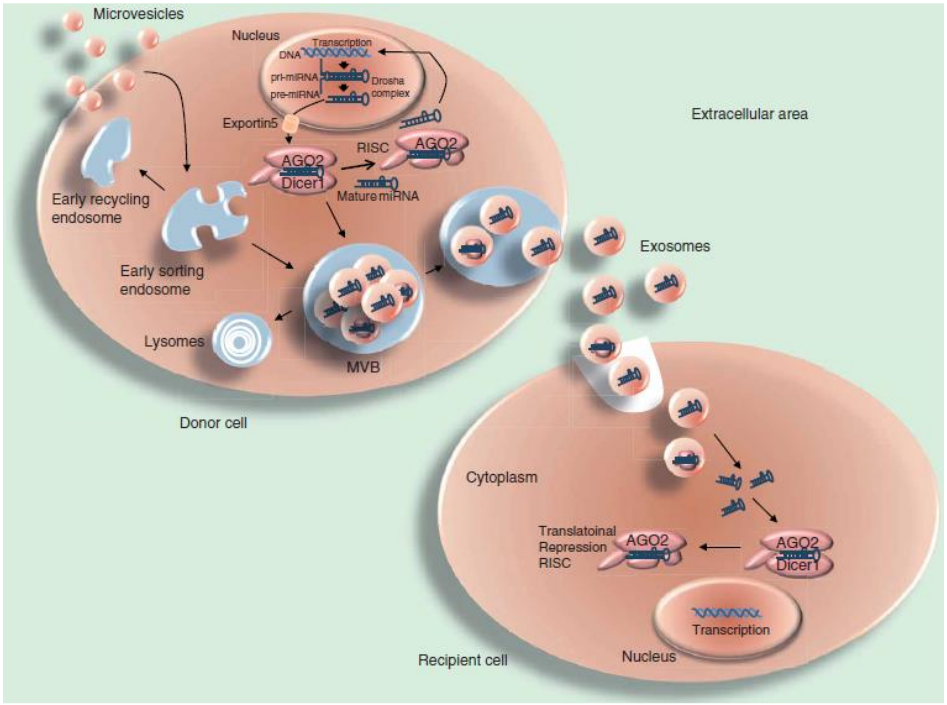

Figure 1.9. Exosome biogenesis and cell-to-cell communication by exosomes (from Schwarzenbach, Expert Rev Mol Diagn, 2015)

Microvesicles fuse with early sorting endosomes. Some of them serve as recycling endosomes back to the cell surface. The other early endosomes mature into MVBs, containing internal luminal vesicles (exosomes). The MVB fuse with the lysosome where they are degraded, or with the plasma membrane allowing the release of exosomes into the extracellular space. The exosomes deliver then their cargos to the recipient cell. In the

recipient cell the uptaken nucleic acids and proteins may manipulate the characteristics of the cell.

1.6.2. Exosomes function

Exosomes are secreted by many cell types, such as neuronal cells, fibroblast cells, adipocytes, intestinal epithelial cells and tumor cell lines (68). It is believed that exosomes influence the physiological and pathological functions of recipient cells by transferring cellular constituents of proteins, RNAs, and lipids to mediate cell-to-cell communication (69, 70). In vitro and in vivo observations corroborate the association of an increased secretion of exosomes with tumor invasiveness and metastasis (71). High concentrations of exosomes were detected in the plasma/serum of BC and epithelial ovarian cancer patients (72, 73). Tumor- and immune cell-derived exosomes carry tumor antigens and can promote immunity (74). Tumor exosomes are also assumed to participate in metastatic dissemination of tumor cells by direct seeding tumor-draining lymph nodes before tumor cell migration (75). Moreover, exosomes can transfer phenotypic traits representing their cells of origin, e.g., a triple-negative character, to secondary cells and confer increased invasiveness to these cells (76). Exosomes also can mediate drug resistance whereas drug-loaded exosomes may act as a next generation drug (77).

1.7. MicroRNAs

1.7.1. MicroRNAs biosynthesis

MicroRNAs (miRNAs) are endogenous non-coding RNAs (ncRNAs) of 18–25 nucleotides in length, and play an important role in inhibiting translation of their target mRNA into protein or in facilitating degradation of their target mRNAs (78).

In the canonical processing, primary miRNA transcripts (pri-miRNAs) are initially transcribed from exons or introns of protein-coding genes. Subsequently, pri-miRNAs are cleaved by the

ribonuclease III (RNase III) type endonuclease DROSHA and its partner proteins (Drosha complex), to generate 70 nucleotides stem loop precursor miRNAs (pre-miRNAs). After being exported to the cytoplasm by Exportin 5, DICER1, another RNase III type endonuclease, processes pre-miRNAs to generate mature miRNAs. One strand of the double-stranded mature miRNA is selectively loaded into the RNA-induced silencing complex (RISC). There, the mature miRNA binds to the 3'untranslated region (3'-UTR) of their target mRNA, and repress its translation or destabilizes it. The other strand of the duplex can either be released and degraded, or loaded into miRISC, to also function as a mature miRNA (79). A subset of miRNAs have also the ability to bind to the open reading frame (ORF) and the 5'untranslated region (5'-UTR) of their target mRNA, to activate or repress its translational efficiency (80, 81) (Figure 1.10).

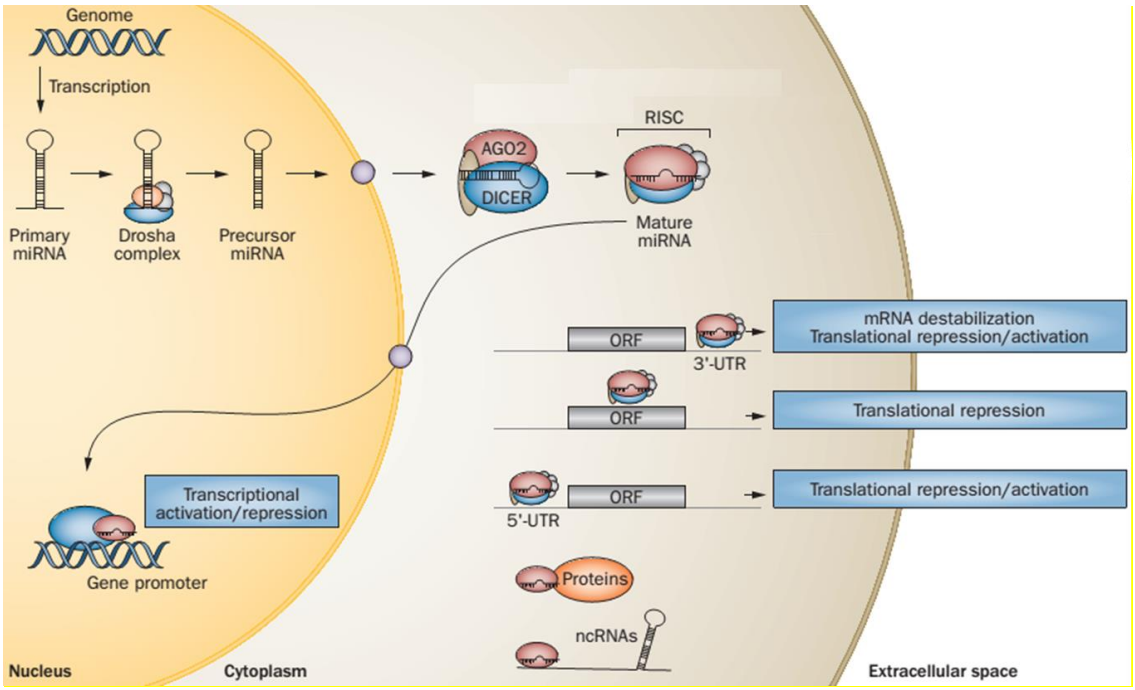

Figure 1.10. Biogenesis and functions of miRNAs (from Schwarzenbach et al., Nat Rev Clin Oncol, 2014)

Pri-miRNA is enzymatically processed by Drosha into pre-miRNA. Then pre-miRNA is transported to the cytoplasm. DICER1 processes pre-miRNA to generate the mature miRNA. One strand of the double-stranded mature miRNA is selectively loaded into the RISC. The mature miRNA affects the translation of their target mRNA by inhibition or destabilization. A

subset of miRNAs can target ORF or 5' UTR of mRNAs, to induce translational repression or translational repression/activation, respectively.

1.7.2. Characteristics of miRNAs

The role of miRNAs in cancer was first reported by Calin et al. in chronic lymphocytic leukaemia (82). So far, it has been reported that miRNAs can be regarded as oncogenic or tumor suppressive miRNAs, such as miR-15/16 cluster, miR-200 family or miR-222/221 cluster (83). Since miRNAs have binding affinity to hundreds of different mRNAs, they regulate numerous signal transduction pathways. Among others, they participate at development, differentiation, proliferation, tumor development and progression (84). In mammals, they are assumed to regulate approximately 50 % of all protein-coding genes (79). MiRNAs can be released into the blood circulation by cell death, such as apoptotic cell and necrotic cell. They can also be released by active secretion of cells then, they are integrated in exosomes. Currently, the selective loading of miRNAs into exosomes that circulate in high amounts in the bloodstream of cancer patients is of growing interest (66, 85).

2. Material and Methods

2.1. Cell lines

For EMF exposure experiment, three BC cell lines MCF-7 (Luminal A BC cell line), MDA-MB-468 (triple-negative BC cell line) and MDA-MB-231 (triple-negative BC cell line), and one normal breast cell line MCF-10A were purchased from American Type Culture Collection (ATCC). MCF-7, MDA-MB-231 and MCF-10A cell lines were authenticated by the Multiplexion GmbH, Heidelberg, on 20/02/2014, while MDA-MB-468 cell lines were authenticated by the Multiplexion GmbH, Immenstaad, on 28/05/2015. Aliquots of cell lines were frozen in liquid nitrogen and fresh cells aliquots of these cell lines were used for this study. MCF-7, MDA-MB-468 and MDA-MB-231 were cultured in DMEM (Dulbecco's Modified Eagle's Medium; PAN Biotech UK Ltd) supplemented with 10 % FCS (fetal calf serum; PAA Laboratories, Cölbe, Germany) under standard conditions (37°C, 5 % CO_2, humidified atmosphere). MCF-10A cells were cultured in DMEM-F12 (Dulbecco's Modified Eagle Medium/Nutrient Mixture F-12; Thermo Fisher Scientific) supplemented with 5 % horse serum (Thermo Fisher Scientific), 100 µg/ml EGF (Epidermal growth factor), 1 mg/ml hydrocortisone, 1 mg/ml cholera toxin, 10 mg/ml insulin and 1 % penicillin/streptomycin under standard conditions (37°C, 5 % CO_2, humidified atmosphere).

2.2. Depletion exosomes from FCS

To avoid quantifying exosomes derived from FCS (86), I depleted exosomes from FCS by the FBS exosome depletion kit II (slurry format; Norgen Biotech, Thorold, Canada) according to the manufacturer's instructions. The depletion is based on Norgen's proprietary resin. Five ml cell culture medium were added to 20 ml FCS followed by the addition of 400 µl EoxC Buffer and 2 ml Slurry E. After mixing well for 10 sec, the mixture was incubated at room temperature (RT) for 10 min. Then, after additional mixing for 10 sec, the mixture was centrifuged for 2 min at 2,000 rpm. The supernatant was transferred into a fresh 50-ml tube

and filtered by a 0.2 µm filter, to get the exosome-depleted FCS filtrate, which was stored at -20°C for future use.

2.3. EMF exposure experiments

For the EMF exposure experiments, I seeded MCF-10A, MCF-7, MDA-MB-468 and MDA-MB-231 in 60 mm dishes (Greiner Bio-one, Frickenhausen, Germany), on the first day. The number of every cell line is indicated in Table 2.1. After 4 hours, the culture medium was changed by medium without FCS. Then each cell line was incubated into two applicators, connected with Somagen® C and D device (CIT Research Sachtleben GmbH, Hamburg, Germany), which provided EMF and standard conditions, respectively). CO_2 were controlled by Pecon CO_2-Controller 2000 and the heat was controlled by a circulation thermostat, Julabo ME-4 (Figure 2.1).

On the second day, I changed the medium by exosome-depleted medium (medium supplemented with Exosome-depleted FCS). Then, cells were exposed with EMF for 30 min per day for 3 days. On the fourth day, after exposure, the supernatant of the cells was taken for the detection of exosomes, whereas the cells were harvested for DNA methylation and hydroxymethylation analyses.

Table 2.1. The number of each cell lines seeded in 60 mm dishes

Cell line	seeding cell(*10^6) in each dish
MDA-MB-231	1
MCF-7	1
MDA-MB-468	2
MCF-10A	1.5

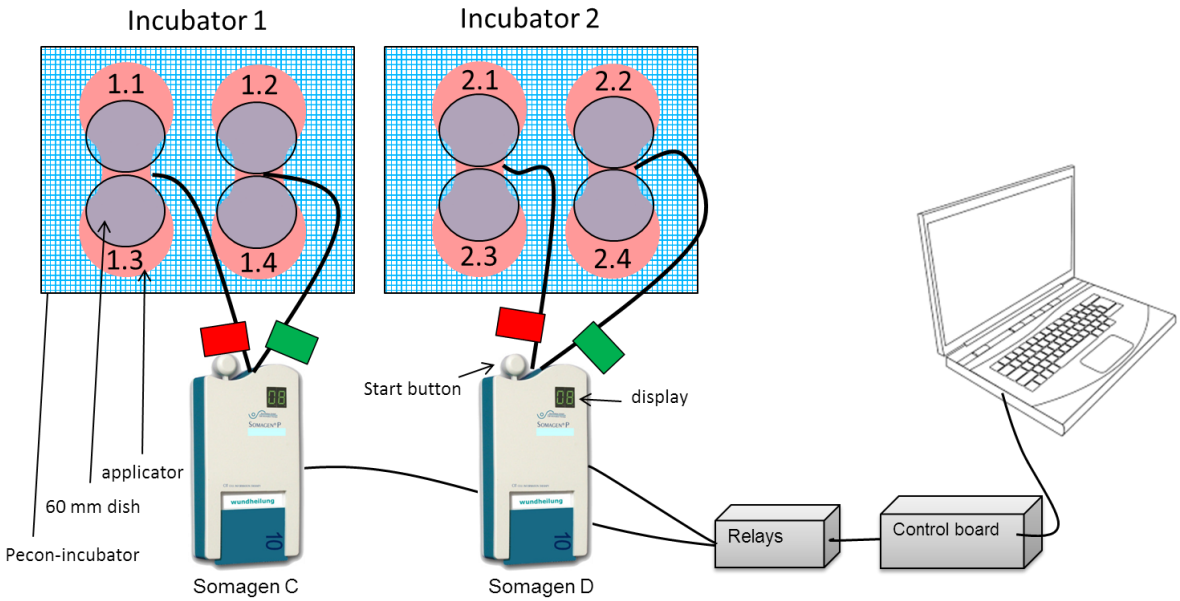

Figure 2.1. Devices in EMF exposure experiments (automated by Teraterm software and supplied by CIT Research Sachtleben GmbH)

Dishes containing 4 different cell lines were put in the incubator and exposed with EMF for 30 min per day. As negative controls, 4 cell lines were also incubated in the second incubator without exposure. All exposure programs were controlled by a computer.

2.4. Counting of cells

After removing the supernatant, the cells were first washed with 1x PBS (phosphate buffered saline; Life Technologies, Paisley, UK) and then, 1 ml pre-warmed accutase (Thermo Fisher Scientific) was added to the cells. MDA-MB-231 cells and MCF-7 cells were incubated at 37°C for 4 min, the MDA-MB-468 cells were incubated at 37°C for 5 min, and MCF-10A cells were incubated at 37°C for 6 min. Five ml pre-warmed complete growth medium were added to resuspend the cells, and the cells were centrifuged at 300×g, 4°C, for 5 min, to remove the cell culture medium. Cell pellets were resuspended by 210 µl cold PBS. Five µl of this cell suspension were diluted, again, in 195 µl PBS, and 5 µl of this dilution were mixed with 5 µl Trypan Blue to count the cell number in a haemocytometer under the microscope (Leica, Wetzlar, Germany), at a 40x enhancement.

2.5. DNA isolation from cell lines

DNA was extracted from exposed and unexposed cells with the QIAamp DNA Kit (QIAGEN, Hilden, Germany). Each harvested cell line was mixed with 20 μl Protease K and 200 μl Buffer AL to lyse the cells. Following vortexing for 15 sec and incubation at 56°C for 10 min, 200 μl 100 % ethanol were added to the mixture. After vortexing for 15 sec, again, the mixture was applied on QIAamp Mini spin columns and centrifuged at 6,000×g, RT, for 1 min, to remove all liquids. Then, 500 μl Buffer AW1 and 500 μl Buffer AW2 were used to remove residual contaminants by centrifugation at 6,000×g, for 1 min, full speed for 3 min. DNA bound at the columns was eluted with 50 μl nuclease-free water. The concentration of DNA was measured using a Qubit dsDNA BR (broad range, 2 to 1000 ng) Assay Kit (Life Technologies, Eugene, USA) on a Qubit 2.0 Fluorometer (Thermo Fisher Scientific). One μl of DNA sample was added to 199 μl of Qubit working solution, whereas 10 μl of Qubit standard were added to 190 μl of standard mixture. Following vortexing for 2-3 sec and incubation at RT for 2 min, the concentration of DNA was measured.

2.6. Detection of DNA methylation and DNA hydroxymethylation

The global levels of DNA methylation and DNA hydroxymethylation were quantified by measuring the amount of 5-mC and 5-hmC in each sample, using the specific ELISA.

2.6.1. Detection of DNA methylation

The Quest 5-mC DNA ELISA Kit (Zymo Research, Irvine, USA) was used for the study of DNA methylation. At first, 100 ng of DNA samples and 5-mC DNA controls (0 %, 5 %, 10 %, 25 %, 50 %, 75 % and 100 %) were mixed with 5-mC coating buffer in a final volume of 100 μl. Then, they were denatured at 98°C for 5 min and incubated on ice for 10 min. The all samples and standards were added to 96-well plates, in duplicates. After incubation at 37°C for 1 h and washing each well for 3 times with 200 μl of 5-mC ELISA Buffer, 200 μl of 5-mC ELISA Buffer were added to each well and incubated at 37ºC for 30 min. Following removing the buffer from the wells, 100 μl of 5-mC ELISA Buffer containing 0.05 μl anti-5-mC and 0.1

µl secondary antibody were added and incubated at 37ºC for 1 h. After washing each well for 3 times with 200 µl of 5-mC ELISA Buffer, again, 100 µl of horse radish peroxidase (HRP) developer were added to each well at RT for 30 min (Figure 2.2). The absorbance of the wells (DNA) was measured at a wavelength of 405 nm on a spectrophotometric plate reader (Tecan, Männerdorf, Switzerland). The amount of 5-mC DNA was calculated according to a linear equation y=a+blnx and by applying the logarithmic second-order regression method.

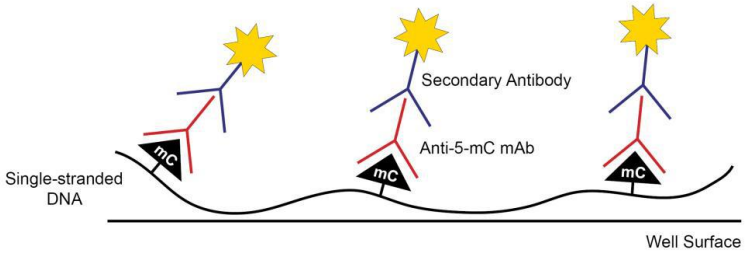

Figure 2.2. The 5-mC DNA ELISA Kit utilizes the indirect ELISA technique in its workflow (supplied by Zymo Research Company)

Denatured, single-stranded DNA samples are coated in 5-mC Coating Buffer on the well surfaces. Anti-5-mC monoclonal antibody (mAb) and the HRP-conjugated Secondary Antibody are prepared in 5-mC ELISA Buffer and added to the wells. Detection of 5-mC DNA occurs after addition of the HRP Developer.

2.6.2. Detection of DNA hydroxymethylation

To determine the global amount of 5-hmC DNA, Quest 5-hmC DNA ELISA Kit (Zymo Research) was utilized. At first, 100 ng of 1 ng/µl anti-5-hmC polyclonal Antibody (pAb) was coated on the bottom of each wells at 37 ºC for 1 h. Then, prepared 100 ng DNA and 5-hmC controls (0 %, 0.03 %, 0.12 %, 0.23 % and 0.55 %) were denatured at 98 ºC for 5 min on a thermocycler. The samples were immediately transferred on the ice and incubated for 10 min. Following washing each well with 200 µl ELISA Buffer for 3 times, 200 µl of ELISA Buffer were added to each well and incubated at 37°C for 30 min. One hundred ng denatured DNA were mixed with ELISA Buffer in a final volume of 100 µl, then coated to each well and incubated at 37ºC for 1 h. 5-hmC DNA was recognized by the antibody 5-hmC pAb. After

washing each well for 3 times with 200 µl of ELISA Buffer, again, 100 µl ELISA Buffer containing 1 µl anti-DNA HRP antibody were added and incubated at 37ºC for 30 min. After 3 further wash steps with 200 µl ELISA Buffer, the addition of 100 µl HRP developer produced a greenish-blue color in the wells (Figure 2.3). The absorbance was measured at a wavelength of 405 nm on a spectrophotometric plate reader (Tecan). The 5-hmC percentage was calculated according to a linear equation y=mx+n and by applying the linear regression method.

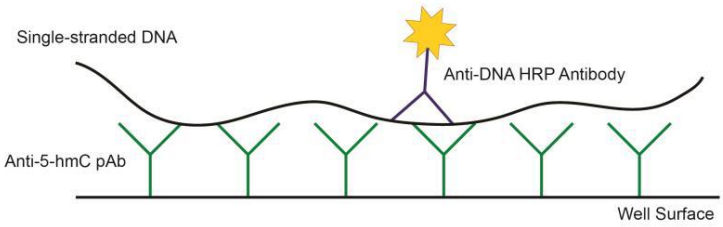

Figure 2.3. Quest 5-hmC™ DNA ELISA Kit is a sandwich-based ELISA format (supplied by Zymo Research Company)

First, anti-5-hmC pAb is coated on the bottom of each well. Denatured single-stranded 5-hmC DNA binds to anti-5-hmC pAb which in turn is recognized by Anti-DNA HRP antibody. Addition of HRP developer produces a greenish-blue color in the wells.

2.7. Isolation of exosomes from cell culture supernatant

Exosome were isolated from cell culture supernatant by using ExoQuick-TC (System Biosciences, Palo Alto, USA) according to the manufacturer's instructions. Briefly, the collected supernatant was centrifuged at 3,000 g for 15 min to remove cells and cell debris. Then, 1 ml ExoQuick-TC Exosome Precipitation Solution was added to 5 ml supernatant and mixed well by flicking the tube. The mixture was incubated overnight at 4°C. On the next day, the biofluid mixture was centrifuged at 1,500 g for 30 min to remove the supernatant. After an additional centrifugation step at 1,500 g for 5 min, the residual liquid was removed. The pellets were resuspended in 50 µl PBS.

2.8. Detection of exosome protein

Exosome protein content was measured using the DC Protein Assay kit (BioRad, Munich, Germany) at a wavelength of 650 nm on a spectrophotometric plate reader (Tecan). A standard curve of 0, 0.15625, 0.3125, 0.625, 1.25, 2.5, 5 and 10 mg/ml BSA (bovine serum albumin; Sigma Aldrich Chemie, Munich, Germany) was applied by the double-dilution method. Then, 3 µl of exosomes and BSA standard samples resuspended in PBS buffer were added to a 96-well plate. Exosome samples were incubated with a mixture of 25 µl Reagent A and stopped with 200 µl Reagent B. After 15 min incubation at RT, the plate was measured at a wavelength of 650 nm on a microplate reader. The obtained OD (optical density) values and the corresponding concentrations of BSA standard protein samples generated a linear equation of $y = mx + n$ by a linear regression analysis. The concentrations of target protein samples were calculated according to this equation.

2.9. Quantification of exosomes by ELISA

The FluoroCet exosome quantitation kit (System Biosciences) is a fluorescence-based, highly sensitive enzymatic assay that measures esterase activity present inside exosomes. At first, a dilution series (1:2, 1:4, 1:8, 1:16, 1:32, 1:64) of FluoroCet standard was used to make the standard curve. Approximately 1 µg protein, equivalent to input exosomes, in a maximal volume of 30 µl per well was used for quantification by the FluoroCet exosome quantitation kit (System Biosciences). Sixty µl of Lysis Buffer were added to 60 µl of the exosome suspension. After 30 min incubation on ice, the proteins were released from the lysed exosomes. Fifty µl of standard or lysed exosome sample, 50 µl working stock of Buffer A and 50 µl of working stock of Buffer B were added to each well of the 96-well plate. Then, the mixture was mixed by gently tapping the sides on the plate, and incubated at RT for 20 min, in dark. After premixing for 30 sec on a spectrophotometric plate reader (Tecan), the exosome concentration was measured at 560 nm excitation and 612 nm emission. Finally, the amounts of exosomes were calculated according to the exosome standard curve,

corresponding to the linear equation of y=mx+n and by applying the linear regression method.

2.10. Study populations and plasma samples

Plasma samples were collected from 111 BC and 42 DCIS patients treated at the University Medical Center Hamburg-Eppendorf, Department of Gynecology. In addition, plasma samples were collected from 39 healthy women who had no history of cancer and were in good health based on self-report. Median age of BC patients, DCIS patients and healthy women was 63 (27 to 92), 58 (30 to 76) and 59 (49 to 71) years, respectively. Plasma samples of BC patients collected directly before surgery and DCIS patients were obtained from November 2013 to September 2016. Those of healthy women were obtained from September 2015 to January 2018. All patients gave written informed consent to access their blood and review their medical records according to the investigational review board and ethics committee guidelines. Regarding blood processing, uniform management concerning the specific, described protocols was performed. Clinicopathological parameters details are described in Table 2.2.

Table 2.2. Clinicopathological parameters of BC patients

BC patients	111
age	63 (27-92)
Recurrence	
yes	46 (41.4 %)
no	65 (58.6 %)
Stage	
1	47 (42.3 %)
2-3	60 (54.1 %)
unknown	4 (3.6 %)
Grading	
G 1-2	60 (54.1 %)
G 3	45 (40.5 %)
unknown	6 (5.4 %)
Histology	
lobular/tubular	21 (18.9 %)
other types	77 (69.4 %)
unknown	13 (11.7 %)
Nodal status	
negative	74 (66.7 %)

positive	31 (27.9 %)
unknown	6 (5.4 %)
Lymph-invasion	
0	74 (66.7 %)
1	27 (24.3 %)
unknown	10 (9 %)
ER status	
negative	28 (25.2 %)
positive	81 (73.0 %)
unknown	2 (1.8 %)
PR status	
negative	35 (31.5 %)
positive	74 (66.7 %)
unknown	2 (1.8 %)
Triple-negative	
yes	24 (21.6 %)
no	85 (76.6 %)
unknown	2 (1.8 %)

2.11. Verification of hemolysis in plasma samples

To avoid analyzing hemolytic plasma samples that may influence the concentrations of exosomal miRNAs, hemoglobin measurements were carried out by spectral analysis. Red blood cells of 7 ml whole blood were lysed by erythrocyte lysis buffer (containing 0.3 M sucrose, 10 mM Tris pH 7.5, 5 mM $MgCl_2$ and 1 % Triton X100). A dilution series (1:1, 1:3, 1:4, 1:6, 1:8, 1:10, 1:12, 1:14, 1:18, 1:20) of lysed red blood cells was prepared in plasma and served as a standard curve for the measurement of hemolysis in all plasma samples. Fifty µl of standard and plasma samples to be analyzed were measured in duplicates on a Microplate reader (Tecan, Männerdorf, Switzerland). Absorbance peaks at 414, 541 and 576 nm were indicative for free hemoglobin, with the highest peak at 414 nm. The higher the absorbance in plasma samples is the higher the degree of hemolysis. The average values were calculated from the duplicates (Figure 2.4).

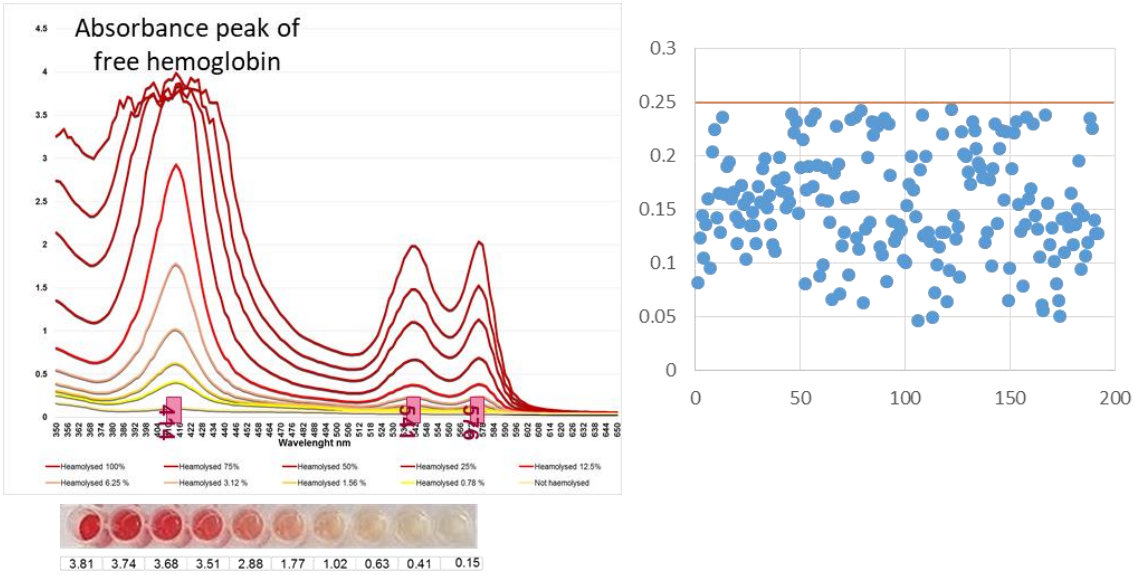

Figure 2.4. Levels of free hemoglobin measured in the plasma samples

Hemolysis was assessed by spectrophotometry at wavelengths from 350 to 650 nm. A dilution series of lysed red blood cells in plasma was prepared (below the chart). The degree of hemolysis was determined based on the OD at 414 nm (absorbance peak of free hemoglobin, called Soret band), with additional peaks at 541 and 576 nm. Samples were classified as being hemolysed if the OD at 414 exceeded 0.25. The integrated scatter plot of plasma samples comprises values from 0.04 to 0.25 indicating that the samples were not hemolysed.

2.12. Extraction of exosomes from plasma

Exosomes were isolated from plasma samples with the ExoQuick kit (BioCat, Heidelberg, Germany). At first, plasma was centrifuged at 3,000 g for 15 min to remove remaining cell debris. Then, 120 µl ExoQuick Exosome Precipitation Solution were added to 500 µl plasma. The plasma-ExoQuick mixture was incubated at 4°C for 30 min and subsequently, centrifuged at 1,500 g, for 30 min and 1,500 g for 5 min to remove the supernatant. The pellet contained the exosomes.

2.13. Western blot

2.13.1. SDS polyacrylamide gel electrophoresis

Sodium dodecyl sulfate polyacrylamide gel electrophoresis (SDS-PAGE) is a technique which separates molecules based on their different molecular weights. When applying current, all SDS-bound proteins which are negatively charged migrate through the gel from the negative electrode towards the positive electrode. Proteins with a lower molecular weight migrate quicker through the gel than those with a higher molecular weight. The gel consists of a concentration and a separation gel. Based on the molecular weight of the proteins, 10 % separation gel was prepared.

Components	10 % separation gel	concentration gel
Double-distilled water	2.5 ml	1.4 ml
30 % Polyacrylamide	3.0 ml	335.0 µl
1 M Tris (pH 6.8)		250.0 µl
1.5 M Tris (pH 8.8)	1.9 ml	
10 % SDS	75.0 µl	20.0 µl
Tetramethylethylenediamine	3.0 µl	2.5 µl
10 % ammonium persulfate	75.0 µl	20.0 µl

About 30 µg exosome proteins were resuspended in 12.5 µl PBS buffer (Life Technologies) mixed with 2.5 µl 6x Loading Buffer (Carl Roth GmbH + Co. KG, Karlsruhe, Germany), and denatured at 95°C for 5 min. Seven µl of PageRulerTM Plus Prestained Protein Ladder (Thermo Scientific) were used to determine the molecular weight of the proteins. The gel was run on a XCell SureLock® Mini-Cell device (Life Technologies) with 1x Laemmli Running Buffer at 125 V for nearly 2 h.

2.13.2. Transfer

The separated proteins on the gel were transferred onto a 0.45 µm polyvinylidene difluoride (PVDF) membrane (Millipore, Billerica, USA) on a XCell II™ Blot Module (Life Technologies). The PVDF membrane was first treated with methanol for 1 min, incubated with double-

distilled water for 3 min, and soaked in transfer buffer for 5 min. Sponge and filter papers were also presoaked with transfer buffer. Sponge, filter paper, gel and membrane were stacked on each other and placed in the cathode core of the XCell II™ Blot Module (Figure 2.5). Transfer buffer were used to fill the cell, and the surrounded area of the cell was filled with cold tap water, which served as cooling unit. The transfer time was at 25 V for 1 h. The components of transfer buffer are as followed:

Components	Volume
48 mM Trisbase	5.81 g
39 mM Glycin	2.93 g
20 % SDS	1.85 ml
MeOH	200 ml
Water until	1 l

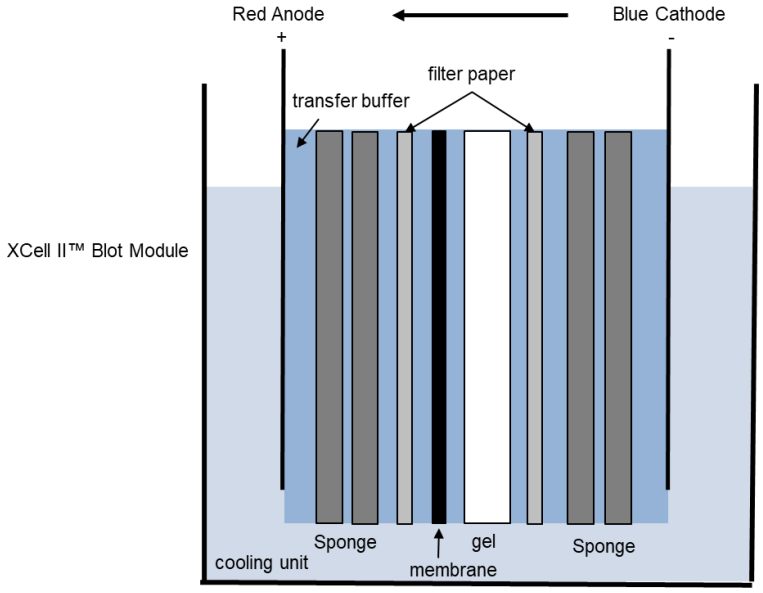

Figure 2.5. Tank transfer apparatus for western blotting

The assembled chamber is filled with transfer buffer, and the outside of the chamber is surrounded with tap water for cooling.

2.13.3. Blocking

For the treatment of the PVDF membrane with the two different first antibodies, specific for CD63 and AGO2 protein which bind to proteins with a molecular weight of 45 kDa and 103

kDa, respectively, the membrane was cut in two parts. To reduce the amount of nonspecific binding, the protein-loaded PVDF membrane for CD63 antibody binding was blocked with 6 % milk solution (6 g in 100 ml TBST buffer) in a 50 ml-tube, at RT for 1 h, and incubated overnight at 4°C with 5 µl (0.5 mg/ml) of the first antibody CD63 (Abgent, San Diego, California, USA) diluted in 5 ml 6 % milk solution. The other part of PVDF membrane for AGO2 antibody binding was blocked with 5 % BSA solution (5 g BSA in 100 ml TBST buffer) at RT for 1 h, and incubated with 5 µl (2 mg/ml) of the miRNA binding protein AGO2 (Takara Bio Inc., Shiga, Japan) diluted in 5 ml 5 % BSA solution.

On the next day, both parts of the PVDF membranes were first washed in 20 ml TBST buffer for 10 min, 3 times. Then the protein-loaded PVDF membrane with CD63 antibody binding was incubated with 2.5 µl of the secondary antibody anti-rabbit immunoglobulins HRP (Dako) diluted in 5 ml of 6 % milk solution at RT for 1 h. The PVDF membrane with AGO2 antibody binding was incubated with 2.5 µl of the secondary antibody anti-mouse immunoglobulins HRP (Dako) diluted in 5 ml of 5 % BSA solution at RT for 1 h. The PVDF membranes were washed in 20 ml TBST buffer for 10 min, 3 times.

2.13.4. Protein detection

HRP (Dako) affects that the luminescent substance luminol (Sigma-Aldrich St.Louis, Missouri, USA) is oxidized by H_2O_2 (Sigma-Aldrich) to luminesce. The components were prepared as followed:

Components	Reagent I	Reagent II
Luminol	100 µl	
p-Coumaric	44 µl	
Tris/HCl pH8.5	1 ml	1 ml
H_2O_2		6 µl
Water	8.85 ml	9 ml

The PVDF membranes were incubated in 10 ml of the mixture of reagent I and reagent II at RT for 4 min, to get the chemiluminescent signals, which were detected with a photosensitive X-ray film (Fuji Safelight Glass, Tokyo, Japan). The exposure time varied from 3 to 5 min

depending of the signal strength. The films were developed on an X-ray film developer Curix60 and scanned on an EPSON perfection V750 PRO device.

2.14. Extraction of miRNAs from exosomes

MiRNAs were extracted from exosomes which were resuspended in 150 µl lysis buffer (Thermo Fisher Scientific, Vilnius, Lithuania) and 50 µl PBS (Life Technologies) by using the TaqMan miRNA ABC Purification Buffer Kit (Thermo Fisher Scientific). To avoid technical variability, 2 µl of 1 nM synthetic non-human cel-miR-39 were added as an exogenous spike in control. According to the manufacturer's instructions, 202 µl lysed exosomal miRNAs were bound to 80 µl anti-miR beads from the TaqMan™ miRNA ABC Purification Bead kit Human panel A (Thermo Fisher Scientific). The mixture was incubated for 40 min by shacking the tube on a Thermomixer at 30°C, 1,200 rpm. Then, the tube was placed on the DynaMagTM-2 magnetic rack for 1 min. After discarding the supernatant, 100 µl Wash Buffer 1 were used to wash the beads twice and then, 100 µl Wash Buffer 2 were used to wash the beads once. Twenty µl Elution Buffer were added to the washed beads, to elute the miRNAs by shacking the tube on a Thermomixer at 70°C, 1,200 rpm for 3 min. The tubes were placed on the DynaMagTM-2 magnetic rack for 1 min. The supernatant contained the eluted miRNAs, which were stored at -80°C for future use.

2.15. Conversion of exosomal miRNAs into cDNA

The reverse transcriptase (RT) is an enzyme which generates complementary DNA (cDNA) from an RNA template. An RNA template and a short primer complementary to the 3' end of the RNA are required for this process.

In my study, RT was carried out using the modified protocol of TaqMan MicroRNA Reverse Transcription kit (Thermo Fisher Scientific). Four µl and 2 µl RNA solution were used for PCR-based TaqMan miRNA array and single TaqMan PCR analyses, respectively. The reaction system and RT-PCR program were carried out as followed. For array cards, Custom

RT Primer Pool (Thermo Fisher Scientific) containing 48 miRNA RT primers was used. For single analysis, 2 µl RT primer of miR-484, cel-miR-39, miR-16, miR-30b and miR-93 mixture diluted in 190 µl TE (Tris-EDTA) formed the RT Primer Pool. The reactions were carried on an MJ Research PTC-200 Peltier Thermal Cycler (Global Medical Instrumentation, Ramsey, Minnesota, USA).

Components	Volume (µl) for array card assay	Volume (µl) for single miRNA analyses
Custom RT Primer Pool	6.0	
RT Primer Pool		4.0
100 mM dNTPs	0.3	0.2
MultiScribe Reverse Transcriptase (50 U/µl)	3.0	2.0
10x Reverse Transcription Buffer	1.5	1.0
Rnase Inhibitor (20 U/µl)	0.19	0.127
Nuclease-free Water	1.01	0.673
RNA	4.0	2.0

PCR program

Temperature	Time
16°C	30 min
42°C	30 min
85°C	5 min
4°C	∞

2.16. Preamplification of cDNA

To increase input cDNA, a preamplification step of cDNA was included. Two µl and 1 µl cDNA solution were used for PCR-based TaqMan miRNA array and single TaqMan PCR analyses, respectively. For array cards, Custom PreAmp Primer Pool (Thermo Fisher Scientific) containing 48 miRNA primers was used. For single analysis, 2 µl TaqMan miRNA primers of miR-484, cel-miR-39, miR-16, miR-30b and miR-93 mixture were diluted in 190 µl TE. The reactions were run on a MJ Research PTC-200 Peltier Thermal Cycler (Global

Medical Instrumentation). A negative control without any templates was included from the starting point of reverse transcription, too.

Components	Volume (µl) for array cards assay	Volume (µl) for single miR analyses
TaqMan® PreAmp Master Mix(2X)	12.5	5.0
Custom PreAmp Primer Pool	3.75	
PreAmp Primer Pool		1.5
Nuclease-free Water	3.75	2.5
RT Product	2.0	1.0

PCR program

Temperature	Time	
95°C	10 min	
55°C	2 min	
72°C	2 min	
95°C	15 sec	} 16 cycles
60°C	4 min	
99.9°C	10 min	
4°C	∞	

2.17. PCR-based TaqMan miRNA arrays

Custom real-time PCR-based TaqMan miRNA array cards (Thermo Fisher Scientific) were used for miRNA profiling. These array cards contained assays for the detection of 45 human miRNAs of interest, 1 endogenous reference miRNAs (miR-484), 1 exogenous reference miRNA (cel-miR-39-3p) for data normalization and 1 assay with an N/A-4343438-Blank (negative control). For the array cards, 45 miRNAs of interest were selected because of their previous description to be clinically relevant and with an exclusive consideration for BC. These miRNAs of interest were then mounted on the array cards by the company Thermo Fisher Scientific and are as follows:

miRBase ID Target sequence

RNU6	GUGCUCGCUUCGGCAGCACAUAUACUAAAAUUGGAACGATACAGAG AAGAUAGCAUGGCCC
miR-1	UGGAAUGUAAAGAAGUAUGUAU
miR-10b	UACCCUGUAGAACCGAAUUUGUG
miR-15b	UAGCAGCACAUCAUGGUUUACA
miR-16	UAGCAGCACGUAAAUAUUGGCG
miR-18a	UAAGGUGCAUCUAGUGCAGAUAG
miR-19a	UGUGCAAAUCUAUGCAAAACUGA
miR-20a	UAAAGUGCUUAUAGUGCAGGUAG
miR-21	UAGCUUAUCAGACUGAUGUUGA
miR-23a	AUCACAUUGCCAGGGAUUUCC
miR-24	UGGCUCAGUUCAGCAGGAACAG
miR-25	CAUUGCACUUGUCUCGGUCUGA
miR-27a	UUCACAGUGGCUAAGUUCCGC
miR-29a	UAGCACCAUCUGAAAUCGGUUA
miR-30b	UGUAAACAUCCUACACUCAGCU
miR-30c	UGUAAACAUCCUACACUCUCAGC
miR-31	AGGCAAGAUGCUGGCAUAGCU
miR-34c	AGGCAGUGUAGUUAGCUGAUUGC
miR-93	CAAAGUGCUGUUCGUGCAGGUAG
miR-99a	AACCCGUAGAUCCGAUCUUGUG
miR-135b	UAUGGCUUUUCAUUCCUAUGUGA
miR-139-3p	GGAGACGCGGCCCUGUUGGAGU
miR-181a	AACAUUCAACGCUGUCGGUGAGU
miR-181c	AACAUUCAACCUGUCGGUGAGU
miR-182	UUUGGCAAUGGUAGAACUCACACU
miR-184	UGGACGGAGAACUGAUAAGGGU
miR-186	CAAAGAAUUCUCCUUUUGGGCU
miR-192	CUGACCUAUGAAUUGACAGCC
miR-196b	UAGGUAGUUUCCUGUUGUUGGG
miR-200a	UAACACUGUCUGGUAACGAUGU
miR-200b	UAAUACUGCCUGGUAAUGAUGA
miR-200c	UAAUACUGCCGGGUAAUGAUGGA
miR-203	GUGAAAUGUUUAGGACCACUAG
miR-205	UCCUUCAUUCCACCGGAGUCUG

miR-210	CUGUGCGUGUGACAGCGGCUGA
miR-212	UAACAGUCUCCAGUCACGGCC
miR-221	AGCUACAUUGUCUGCUGGGUUUC
miR-222	AGCUACAUCUGGCUACUGGGU
miR-301	CAGUGCAAUAGUAUUGUCAAAGC
miR-375	UUUGUUCGUUCGGCUCGCGUGA
miR-451	AAACCGUUACCAUUACUGAGUU
miR-483-5p	AAGACGGGAGGAAAGAAGGGAG
miR-489	GUGACAUCACAUAUACGGCAGC
miR-492	AGGACCUGCGGGACAAGAUUCUU
miR-511	GUGUCUUUUGCUCUGCAGUCA

For miRNA array analyses, the protocol of Thermo Fisher Scientific was modified as followed:

Components	Volume (µl)
TaqMan Universal Master Mix II	56.25
PreAmp product	2
Nuclease-free Water	54.2

The PCR array cards were run on a 7900 HT Fast Real-Time PCR System (Applied Biosystems).

PCR program

Temperature	Time	
95°C	10 min	
95°C	15 sec	40 cycles
60°C	1 min	

2.18. Single TaqMan PCR analyses of miR-16, miR-30b and miR-93

For quantitative real-time PCR, the TaqMan miRNA assays (Thermo Fisher Scientific) for miR-484 and miR-39 (reference miRNAs), and miR-16, miR-30b and miR-93 were used. Quantitative real-time PCR reaction was performed on a C1000 Touch real-time PCR device

(Bio-Rad, Hercules, California, USA). The reaction system and real-time PCR program were carried out as followed:

Components	Volume (µl)
TaqMan Universal Master Mix II	5.0
PreAmp product	0.25
TaqMan MicroRNA Assay	0.5
Nuclease-free Water	4.4

PCR program

Temperature	Time	
95°C	10 min	
95°C	15 sec	40 cycles
60°C	1 min	

2.19. Data normalization and statistical analyses

-- EMF experiment

The Microsoft Excel 2010 was used, to make bar charts and box plots. The measured data of EMF-exposed cell lines were divided by those of unexposed cell lines means. The resulted value 1 means no change, the value lower than 1 means decrease and the value higher than 1 means increase in cell number, DNA methylation, hydroxymethylation and exosome concentration.

-- MiRNA experiment

Data analyses were performed using the Thermo Fisher Scientific Analysis Software, Relative Quantification Analysis Module, version 3.1 (www.aps.thermofisher.com), and SPSS software package, version 22.0 (SPSS Inc. Chicago, IL).

As there is no consensus on a reference miRNA for data normalization, the exosomal miR-484 and cel-miR-39 were chosen as an endogenous and exogenous reference gene, respectively. MiR-484 showed the smallest variation between healthy individuals, DCIS patients and BC patients. The inter-individual variability of the efficiency of my procedures

was controlled by spiking in of cel-miR-39-3p. The obtained data of the miRNA expression levels were calculated by the ΔCq method as follows: ΔCq = mean Cq value (reference cel-miR-39 + miR-484) − mean Cq value (miRNA of interest). The Thermo Fisher Scientific Analysis Software was used for performing hierarchical clustering (heat map) and volcano plots. Distances between samples and assays were calculated for hierarchical clustering based on the ΔCq values using Pearson's Correlation. Clustering method was average linkage. Subsequently, the relative expression data were 2^(ΔCq) transformed in order to obtain normal distribution data. The confidence of 2^(ΔCq) data were verified by amplification curves, and Cq confidence (0-1, whereby 1 refers to the highest confidence). My data showed a Cq confidence of 0.95. Values below 0.95 were discarded. Statistical differences of exosomal miRNA expressions between healthy controls, DCIS patients and BC patients were calculated using two-tailed student t-test and depicted as a volcano plot. The correlations of plasma levels of exosomal miRNAs with clinical parameters were calculated by using two-tailed student t-test. A p-value <0.05 was considered as statistically significant.

3. Results

3.1. Investigations of the effects of EMFs on BC cell lines

3.1.1. Work flow

Four cell lines MDA-MB-231, MDA-MB-468, MCF-7 and MCF-10A were used for EMF exposure experiments (Table 2.1). After 3 days EMF exposure, the cell culture supernatant was prepared for the quantification of exosomes. The cells were harvested for epigenetic analyses, such as the detection of DNA methylation and hydroxymethylation. At first, the cell number of each cell lines was counted. For finding the appropriate frequency of EMF for inhibition of BC cell growth and exosome release, as well as changes in epigenetics in BC cells, 8 different frequencies of EMF were applied in the experiments (Figure 3.1).

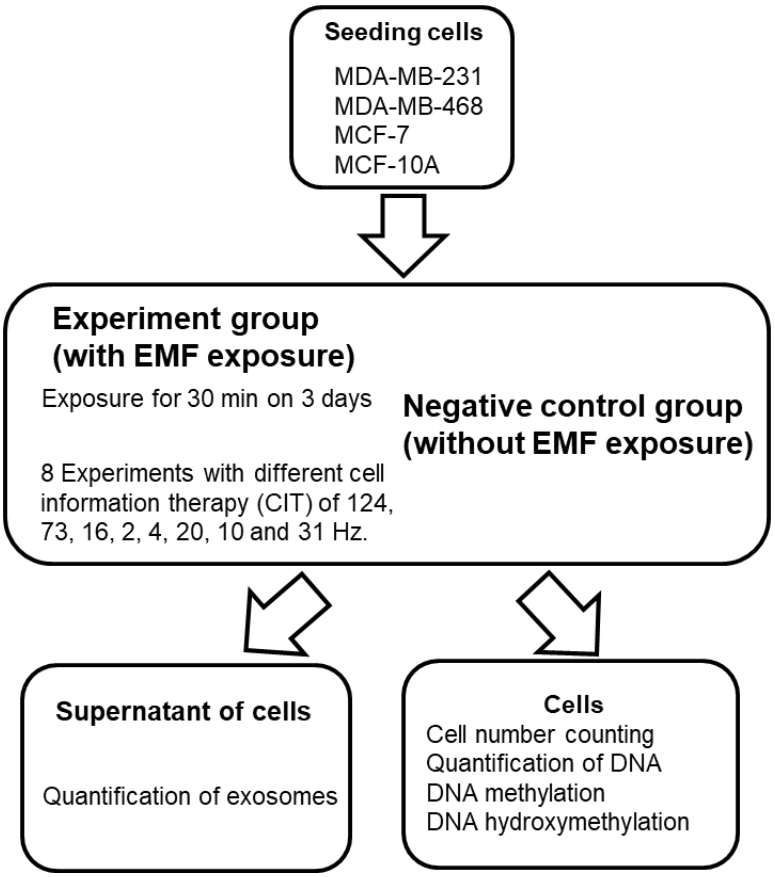

Figure 3.1. Workflow of the present study

3.1.2. The impact of EMF exposure on cell number

Different frequencies of EMF were applied, to inhibit cell growth. However, the impact of EMF was only small. The best inhibiting effect of EMF was observed on MDA-MB-231 cell count in experiment IV with CIT program #2 (2 Hz, Figure 3.2).

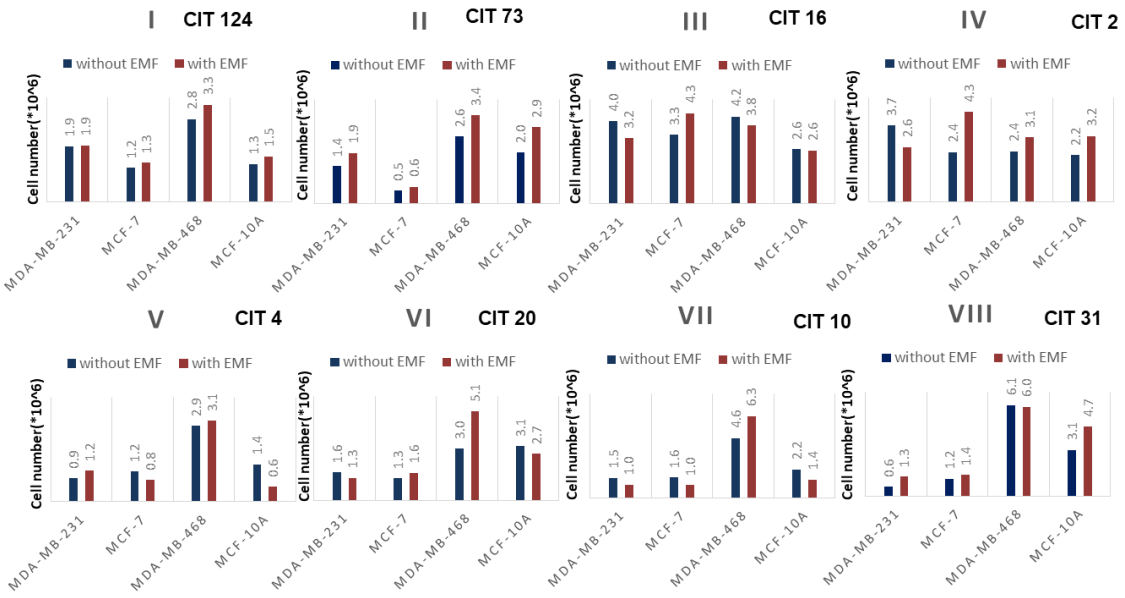

Figure 3.2. The cell numbers of 4 cell lines in EMF exposure experiments

Blue columns present the numbers of cell lines without EMF exposure. In contrast, red columns present the numbers of cell lines exposed with EMF of different frequencies.

CIT 124, program #124 with 124 Hz and so on.

3.1.3. The impact of EMF exposure on 5-mC DNA

Different frequencies of EMF were applied, to demethylate BC cells. However, the impact of EMF was only small. The best inhibiting effect on DNA methylation by EMF was observed in experiment VII with CIT program # 10 (10 Hz, Figure 3.3).

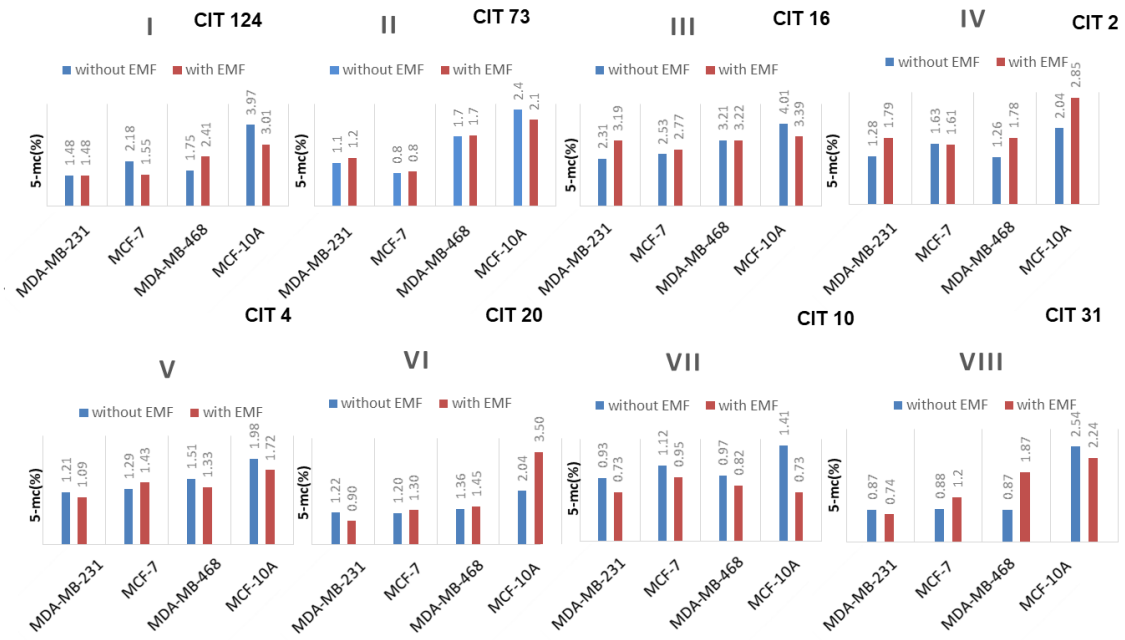

Figure 3.3. The levels of 5-mC DNA of 4 cell lines in EMF exposure experiments

Blue columns present the levels of 5-mC DNA without EMF exposure. In contrast, red columns present the levels of 5-mC DNA lines exposed with EMF of different frequencies.

3.1.4. The impact of EMF exposure on 5-hmC DNA

Different frequencies of EMF were applied, to induce 5-hmC DNA. However, the impact of EMF was variable. The best stimulatory effect on DNA hydroxymethylation by EMF was observed in MCF-7 cell line in experiment I with CIT program #124 (124 Hz). The best overall effect of EMF was in experiment VIII with CIT program #31 (31 Hz, Figure 3.4).

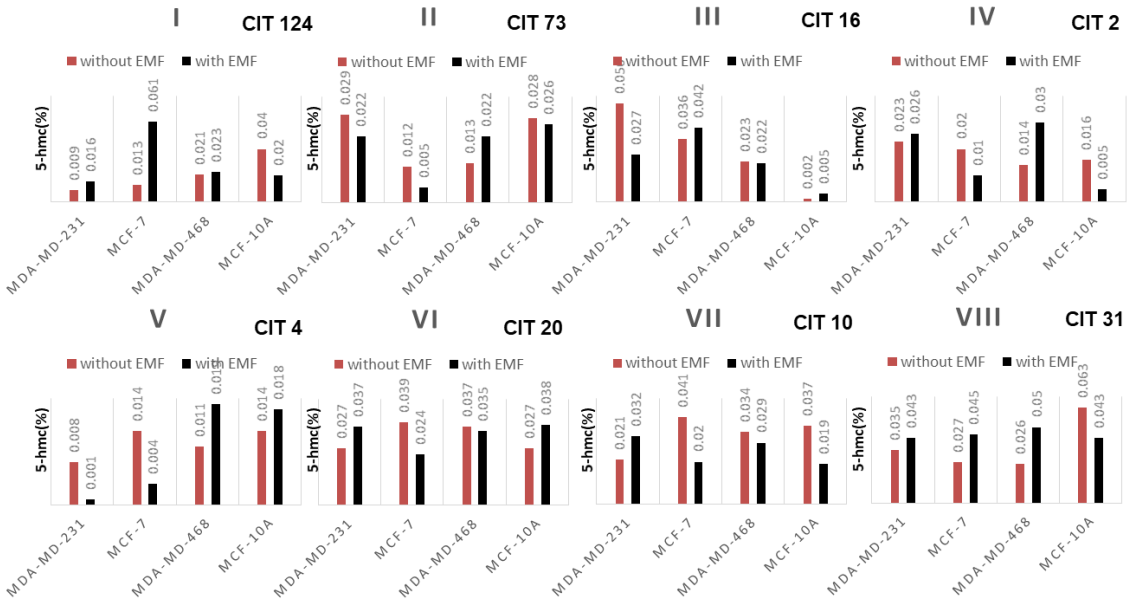

Figure 3.4. The levels of 5-hmC DNA of 4 cell lines in EMF exposure experiments

Blue columns present the levels of 5-hmC DNA without EMF exposure. In contrast, red columns present the levels of 5-hmC DNA lines exposed with EMF of different frequencies.

3.1.5. The impact of EMF exposure on the levels of exosomes in cell lines

Different frequencies of EMF were applied, to decrease the levels of exosome. However, the impact of EMF was only small. The best inhibiting effect on exosome secretion by EMF was observed on MCF-7 cell line in experiment I with CIT program #124 (124 Hz). The best overall effect of EMF was in experiment VII with CIT program #10 (10 Hz, Figure 3.5).

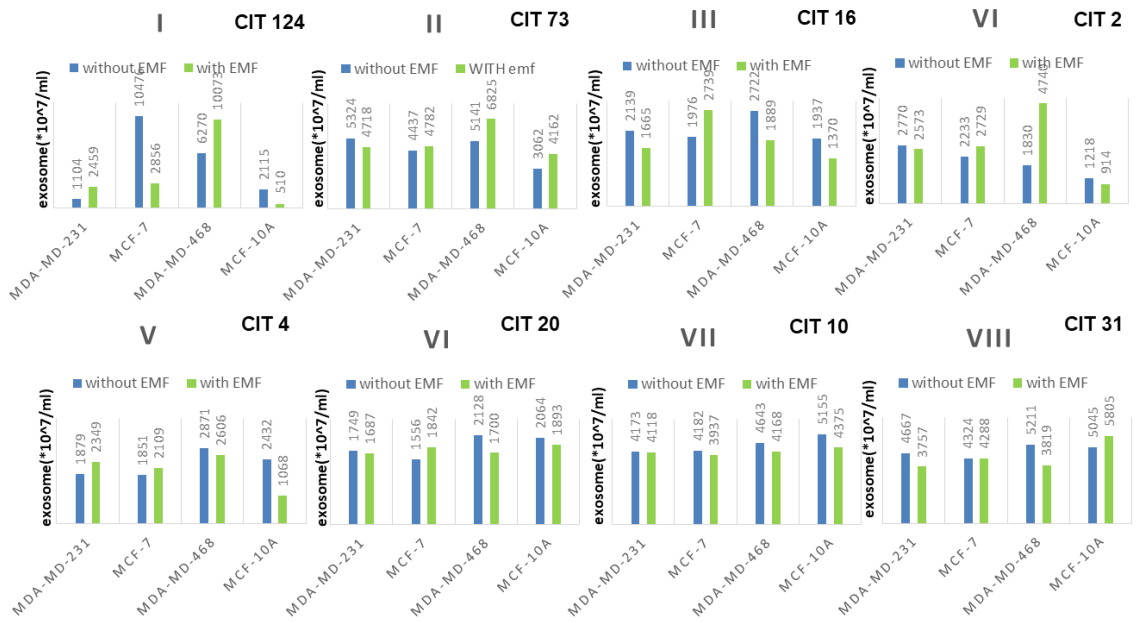

Figure 3.5. The concentrations of exosomes released from 4 cell lines in EMF exposure experiments

Blue columns present the concentrations of exosomes without EMF exposure. In contrast, green columns present the concentrations of exosomes lines exposed with EMF of different frequencies.

3.1.6. Repetition of experiments II and VIII

Additionally, I repeated experiments II (73 Hz) and VIII (31 Hz) for 3 times because of their best impacts by EMF on cell lines. In the repeated experiments II (73 Hz), cell numbers of all cell lines increased more or less after exposure with EMF (Figure 3.6.A). However, EMF had no impact on 5-mC DNA in all cell lines (value = 1, Figure 3.6.B). EMF had different impacts on 5-hmC DNA in the 4 cell lines. In MDA-MB-468 cell line, the levels of 5-hmC DNA increased after exposure with EMF. In MCF-7 cell line, the levels of 5-hmC DNA decreased after exposure with EMF (Figure 3.6.C). The levels of exosomes decreased somewhat in MDA-MB-231 and MCF-7 cell lines as well as increased in MDA-MB-468 and MCF-10A cell lines (Figure 3.6.D).

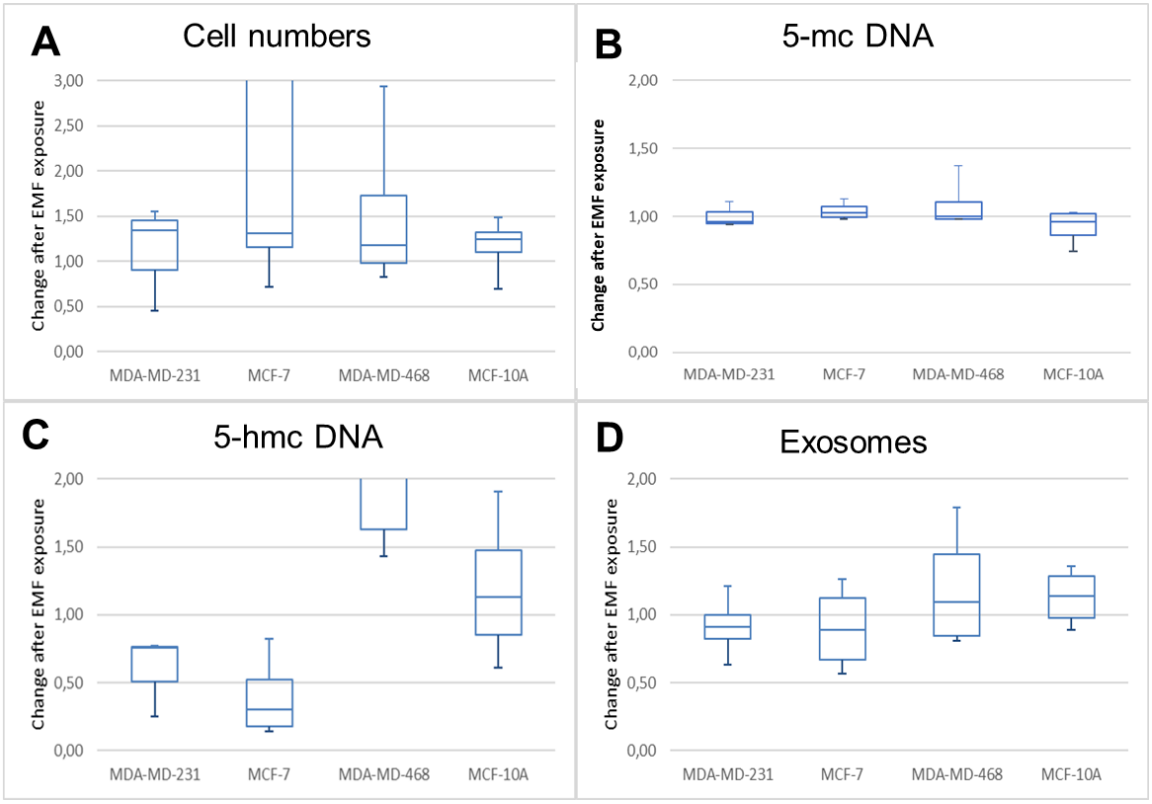

Figure 3.6. The impact of EMF exposure on 4 cell lines in experiments II (73 Hz)

The box plots show the changes in cell numbers (A), 5-mC DNA (B), 5-hmC DNA (C) and levels of exosomes (D) with the deviations from 4 experiments in 4 cell lines after exposure with EMF. The values on Y-axis mean the changes after exposure with EMF: 1, no change; <1, decrease; >1, increase.

In experiments VIII, I found increased cell numbers of all cell lines except the MDA-MB-468 cell line after exposure with EMF (Figure 3.7.A). However, EMF still had no impact on 5-mC DNA in all cell lines (Figure 3.7.B). In MDA-MB-468 cell line, the levels of 5-hmC DNA increased obviously after exposure with EMF (Figure 3.7.C). In MCF-10A cell line, the levels of exosomes increased after exposure with EMF (Figure 3.7.D).

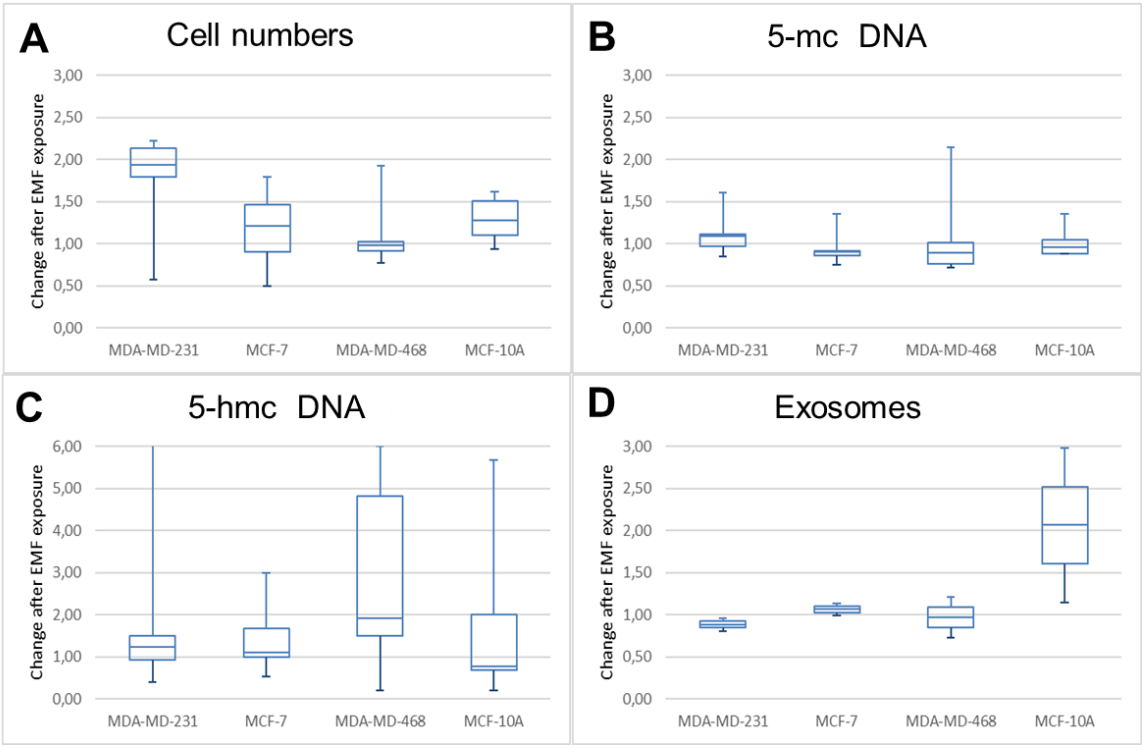

Figure 3.7. The impact of EMF exposure in 4 cell lines in experiments VIII (31 Hz)

The box plots show the changes in cell numbers (A), 5-mC DNA (B), 5-hmC DNA (C) and levels of exosomes (D) after exposure with EMF in 4 cell lines. The values on Y-axis mean the changes after exposure with EMF: 1, no change; <1, decrease; >1, increase.

3.2. Circulating exosomal microRNAs in blood of BC patients

3.2.1. Work flow

At first, real-time PCR-based miRNA array cards containing 45 miRNAs (plus 2 reference miRNAs and an empty control) were used to quantify miRNAs in exosomes derived from plasma samples of 32 BC patients, 8 DCIS patients and 8 healthy women. Then, three significantly deregulated exosomal miRNAs (miR-16, miR-30b and miR-93) derived from these array analyses were selected for single TaqMan real-time PCR assays using exosomes from plasma of 111 BC patients, 42 DCIS patients and 39 healthy women. The relative miRNA data normalized by the endogenous miR-484 and exogenous cel-miR-39 were statistically evaluated, and compared among the cohorts and with the clinical

parameters of the BC patients. Exosomes were verified in 3 BC patients, 1 DCIS patient and 1 healthy woman by a Western blot. Figure 3.8 summarizes the single steps of the workflow.

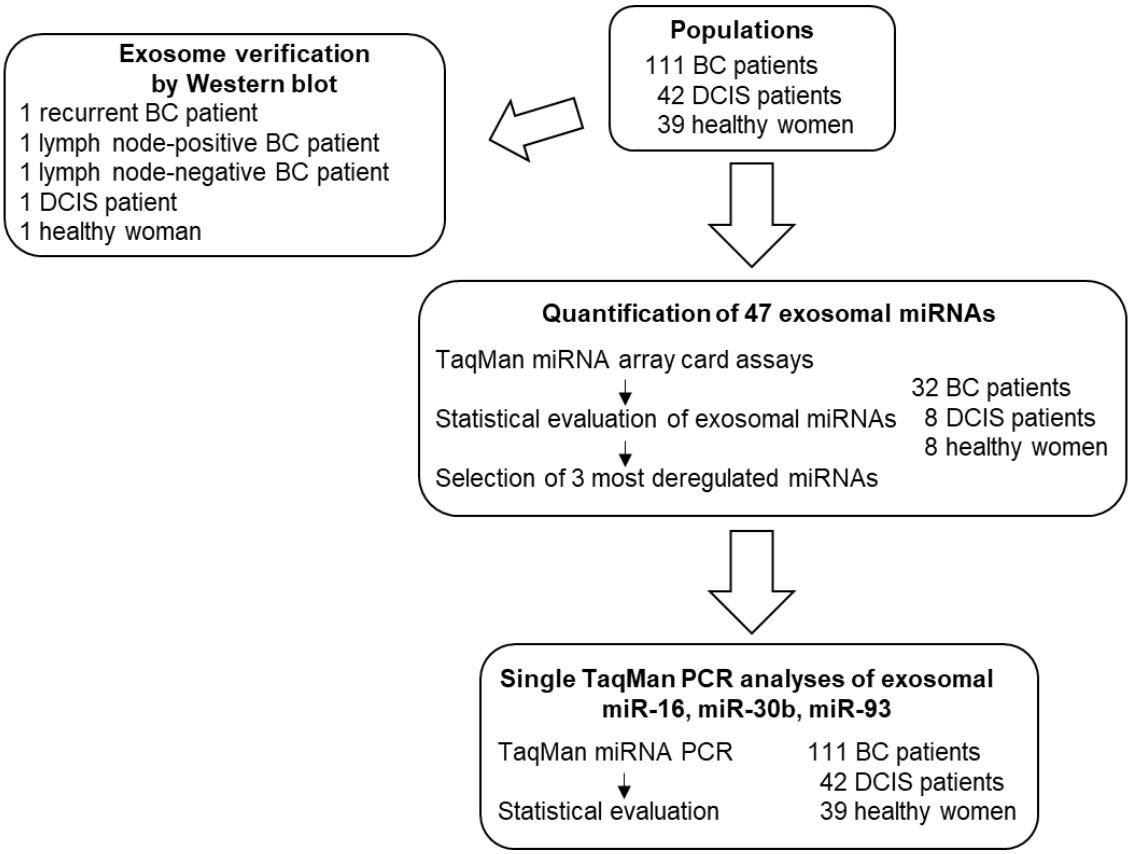

Figure 3.8. Workflow of the present study

3.2.2. Verification of exosomes

Prior to quantification of exosomal miRNAs, the extractions of exosomes from a healthy woman and a patient with DCIS, lymph node-negative BC, lymph node-positive BC and recurrent BC were verified on a Western Blot using antibodies specific for the exosomal marker CD63 and the miRNA binding protein AGO2. As shown by the 45 kDa and 103 kDa band on the blot, the CD63-specific antibody recognized non-lysed exosomes in the pellet, whereas the AGO2-specific antibody did not detect AGO2 protein which is bound to cell-free miRNAs in the exosome pellet, respectively. Conversely, exosome- and cell-free AGO2-bound miRNAs could only be found in the supernatant (Figure 3.8). These findings show that the exosome fraction may be pure and devoid of cell-free miRNAs. However, they do not

exclude that the exosomes may contain traces of contaminations of AGO2-bound miRNAs that due to the sensitivity of the Western blot were not detectable (Figure 3.9).

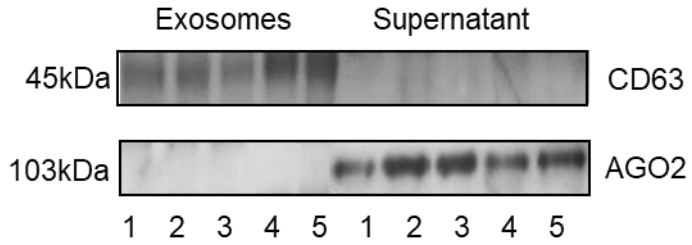

Figure 3.9. Verification and quantification of exosomes.

Exosomes were precipitated from plasma of a healthy woman, DCIS patient and BC patients by the agglutinating agent ExoQuick and analyzed by Western blots using antibodies specific for the exosomal marker CD63, and the miRNA-associated AGO2 protein. The Western blots show representative examples of exosomes, devoid of cell-free miRNAs. Lane 1, healthy woman; lane 2, DCIS patient; lane 3, lymph node-negative BC patient; lane 4, lymph node-positive BC patient; lane 5, recurrent BC patient.

3.2.3. MiRNA profiling in exosomes of BC and DCIS patients

Next, I carried out a quantitative TaqMan real-time PCR-based microarray with cards containing 45 different miRNAs (plus 3 references), to determine the miRNA expression profiles in exosomes derived from the plasma of 32 BC (16 primary and 16 recurrent) patients, 8 DCIS patients and 8 healthy women (Figure 3.8). I selected the miRNAs for the assembly of the 48-microarray cards due to their oncogenic/tumor suppressive function in BC as described in the literature (PubMed) and in our previous studies (72, 87-90). The selected miRNAs are listed in Materials and Methods. Then, a similarity matrix was generated containing all pairwise similarities of the exosome samples from plasma of BC patients, DCIS patients and healthy controls. To detect potential clusters in rows (miRNAs) and columns (plasma samples) of the normalized expression matrix, hierarchical clustering was carried out. The relative up- and downregulated miRNAs are indicated by different nuances of red and green, respectively (heat map, Figure 3.10).

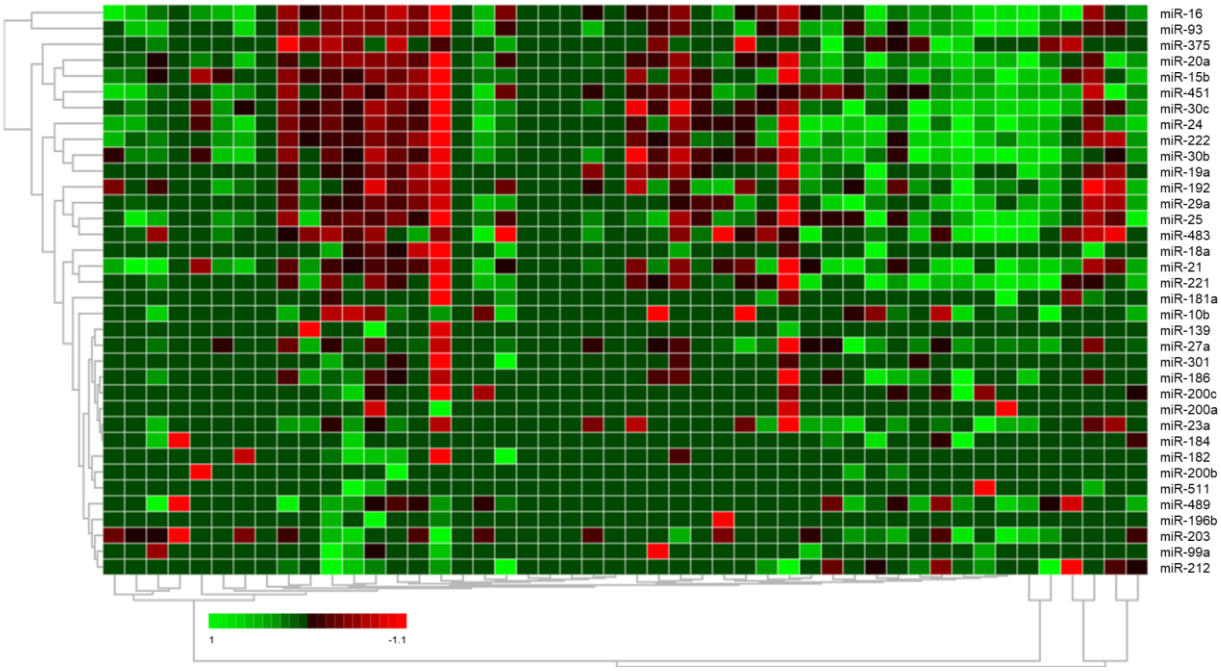

Figure 3.10. Hierarchical cluster of 47 exosomal miRNAs

The heat map is derived from data of the miRNA array assays which were carried out by quantitative real-time PCR based array cards mounted with assays for detection of 47 different miRNAs and using exosome samples from plasma of 32 BC patients, 8 DCIS patients and 8 healthy women. The colored representation of samples and probes is ordered by their similarity. The red and green colors indicate that the ΔCq value is below (relatively high expression) and above (relatively low expression levels) the median of all ΔCq values in the study, respectively. On top: clustering of samples. On the right side: clustering of probes. The scale bar provides information on the degree of regulation.

As shown in the Volcano plot, exosomal miR-16 (p=0.014) and miR-93 (p=0.038) were upregulated in primary BC patients compared with healthy women (Figure 3.11.A). The levels of 6 exosomal miRNAs differed between primary and recurrent BC. In particular, the levels of miR-20a (p=0.008) and miR-30b (p=0.008) were higher in exosomes from primary than recurrent BC patients (Figure 3.11.B). In each case, the levels of 9 miRNAs could distinguish DCIS from BC patients (Figure 3.11.C) and healthy women (Figure 3.11.D). I selected exosomal miR-16, miR-30b and miR-93 for single TaqMan PCR assays, because

the increased levels of miR-16 in DCIS patients compared with healthy women (p=0.001) decreased in all BC patients (p=0.004) and recurrent patients compared with DCIS patients (p=0.001). Alike, the levels of miR-30b were higher in DCIS patients than healthy women (p=0.038) and decreased in all BC patients (p=0.037) and recurrent BC patients in comparison with DCIS patients (p=0.003). The levels of miR-93 were also higher in DCIS patients than healthy women (p=0.001), but decreased in all BC patients (p=0.007) and recurrent BC patients compared with DCIS patients (p=0.002, Figure 3.11, Table 3.2).

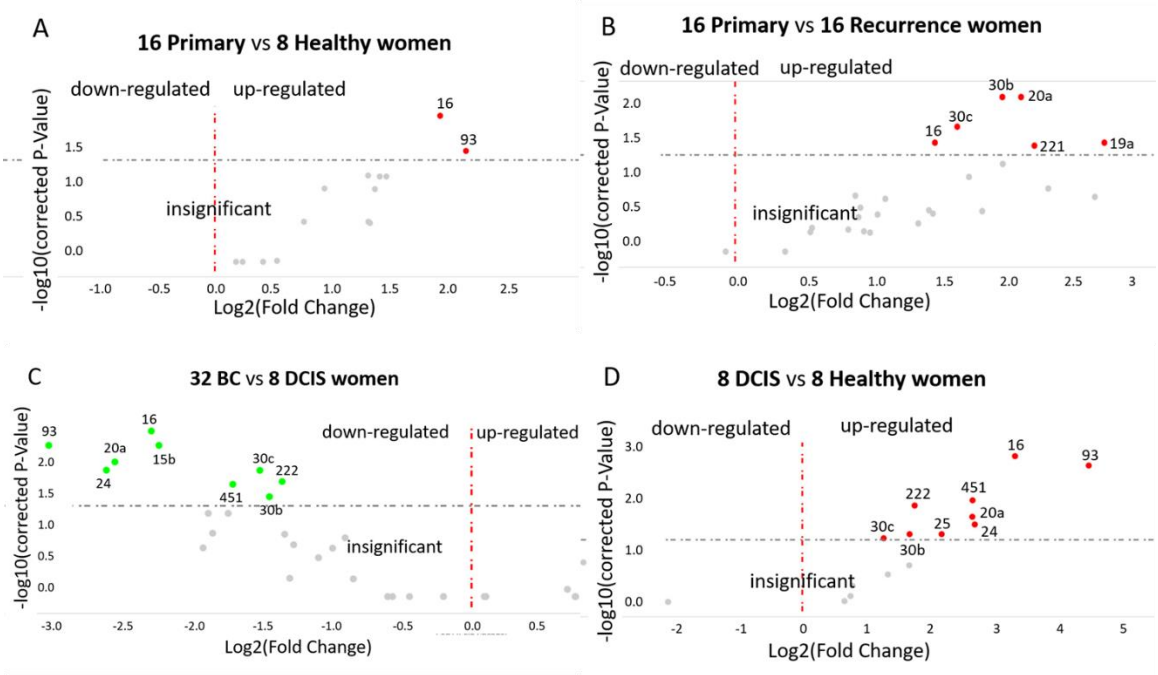

Figure 3.11. Volcano plots of exosomal miRNAs

The plots were drawn for comparison of exosomal miRNA levels in plasma of 16 primary BC patients with those of 8 healthy women (A) and 16 primary BC patients with recurrence (B) as well as of 32 BC patients with 8 DCIS patients (C), and of 8 DCIS patients with 8 healthy women (D). The Log2 fold changes are plotted on the x-axis and the negative log10 p-values are plotted on the y-axis. The left side shows downregulated exosomal miRNAs (green dots). The right side shows upregulated exosomal miRNAs (red dots). Under the dashed horizontal line there are non-deregulated miRNAs (grey dots).

Table 3.2. Summary of the deregulated exosomal miRNAs using array cards containing 48 miRNAs

Populations	No.		miR-15b	miR-16	miR-20a	miR-24	miR-25	miR-30b	miR-30c	miR-93	miR-222	miR-451
All BC vs. Healthy	32 vs. 8	fold change	0.5	2.0	1.1	1.1	1.9	1.2	0.8	**2.7**	1.3	1.9
		p-value	0.576	0.093	1.0	1.0	0.224	1.0	1.0	**0.012**	0.466	0.174
Primary vs. Healthy	16 vs. 8	fold change	1.1	**3.7**	2.5	2.4	2.7	2.6	1.7	**4.3**	1.9	2.4
		p-value	1.0	**0.014**	0.118	0.307	0.081	0.081	0.307	**0.038**	0.116	0.079
Recurrence vs. Healthy	16 vs. 8	fold change	0.3	1.3	0.6	0.6	1.4	0.7	0.5	1.2	1.0	1.6
		p-value	0.171	0.695	0.307	0.433	0.678	0.319	0.080	0.116	1.0	0.373
Primary vs. Recurrence	16 vs. 16	fold change	3.4	**2.8**	**4.4**	4.0	1.9	**4.0**	**3.2**	2.1	1.9	1.5
		p-value	0.099	**0.034**	**0.008**	0.066	0.256	**0.008**	**0.021**	0.318	0.177	0.480
DCIS vs. Healthy	8 vs. 8	fold change	2.5	**9.8**	**6.2**	**6.4**	**4.5**	**3.2**	**2.4**	**21.8**	**3.3**	**6.2**
		p-value	0.267	**0.001**	**0.016**	**0.024**	**0.038**	**0.038**	**0.046**	**0.001**	**0.010**	**0.007**
All BC vs. DCIS	32 vs. 8	fold change	**0.2**	**0.2**	**0.2**	**0.2**	0.4	**0.4**	**0.4**	**0.1**	**0.4**	**0.3**
		p-value	**0.007**	**0.004**	**0.012**	**0.015**	0.557	**0.037**	**0.016**	**0.007**	**0.023**	**0.025**
Primary vs. DCIS	16 vs. 8	fold change	0.5	0.4	0.4	0.4	0.6	0.8	0.7	**0.2**	0.6	0.4
		p-value	0.320	0.065	0.229	0.324	0.613	1.0	0.648	**0.044**	0.273	0.082
Recurrence vs. DCIS	16 vs. 8	fold change	**0.1**	**0.1**	**0.1**	**0.1**	0.3	**0.2**	**0.2**	**0.1**	**0.3**	**0.3**
		p-value	**0.002**	**0.001**	**0.002**	**0.003**	0.082	**0.003**	**0.002**	**0.002**	**0.008**	**0.017**

The table only shows those exosomal miRNAs which were significantly deregulated in a patient group/subgroup. The significant p-values with the corresponding fold changes of exosomal miRNAs are in bold.

Then, I analyzed the selected miR-16, miR-30b and miR-93 in exosomes from plasma of 111 BC patients, 42 DCIS patients and 39 healthy women by single TaqMan real-time PCR assays. The higher levels of exosomal miR-16 in all BC patients than in healthy women (p=0.034) were not observed in primary BC patients, but in recurrent patients (p=0.016), indicating that this increase was possibly linked with recurrence. The deregulated levels of miR-16 in DCIS patients compared with those of healthy women and all BC patients were borderline (p=0.047). No changes in the levels of exosomal miR-30b could be observed in primary and recurrent BC patients, as well as in DCIS patients (Table 3.3, Figure 3.12). These findings were different from the data derived from the analyses using the array cards, suggesting that the number of patients and healthy women was too low in the array analyses to get robust p-values. However, the significant increase in the levels of exosomal miR-93 in

DCIS patients using array cards could also be found in these patients by single PCR assays (p=0.001, Table 3.3, Figure 3.12.).

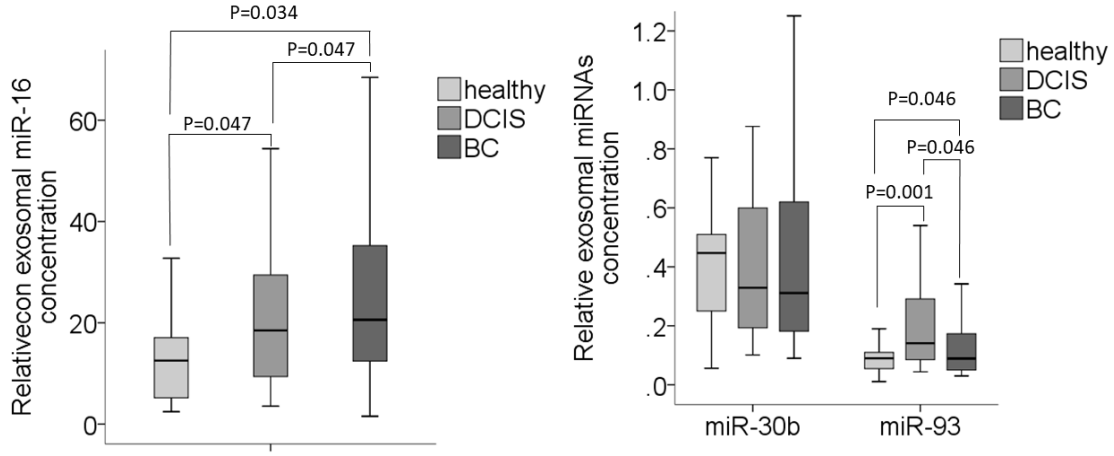

Figure 3.12. Exosomal miRNA levels in BC patients, DCIS patients and healthy women

The both box blots show the plasma levels of exosomal miR-16, miR-30b and miR-93 in 39 healthy women, 42 DCIS patients and 111 BC patients. P-values are indicated.

Table 3.3. Different enrichments of miR-16, miR-30b and miR-93 in exosomes.

Populations	No.		miR-16	miR-30b	miR-93
All BC vs. healthy	111 vs. 39	fold change p-value	**2.1** **0.034**	0.9 0.903	**1.2** **0.046**
Primary vs. Healthy	65 vs. 39	fold change p-value	1.9 0.067	1.1 0.538	1.4 0.057
Recurrence vs. Healthy	46 vs. 39	fold change p-value	**2.5** **0.016**	0.7 0.195	1.1 0.345
Recurrence vs.Primary	46 vs. 65	fold change p-value	1.3 0.214	**0.7** **0.034**	0.8 0.151
DCIS vs. healthy	42 vs. 39	fold change p-value	**1.8** **0.047**	0.9 0.870	**2.0** **0.001**
All BC vs. DCIS	111 vs. 42	fold change p-value	**1.2** **0.047**	1.0 0.732	**0.6** **0.046**
Primary vs. DCIS	65 vs. 42	fold change p-value	1.1 0.326	1.2 0.707	0.7 0.465
Recurrence vs. DCIS	46 vs. 42	fold change p-value	**1.4** **0.029**	0.8 0.224	**0.5** **0.005**
BC subtypes					
Histology lobular/tubular vs. other types	21 vs. 77	fold change p-value	1.1 0.785	**0.7** **0.024**	1.3 0.300

ER status positive vs. negative	81 vs. 28	fold change	**1.5**	1.1	1.5
		p-value	**0.004**	0.537	0.201
PR status positive vs. negative	74 vs. 35	fold change	**1.4**	1.2	**1.9**
		p-value	**0.008**	0.953	**0.010**
Triple-negative yes vs. no	24 vs. 85	fold change	**0.7**	0.8	0.7
		p-value	**0.012**	0.891	0.296

Significant p-values with the corresponding fold changes of exosomal miRNAs are in bold.

3.2.4. Association of exosomal miR-16, miR-30b and miR-93 with the clinicopathological parameters of BC patients

The statistical comparison with clinical data showed that the levels of exosomal miR-16 are associated with the receptor status of BC patients. The levels were higher in ER-positive BC patients (p=0.0001) and PR-positive BC patients (p=0.0001, Figure 3.13.A) than in healthy women. Alike, the levels of miR-16 were higher in ER-positive BC patients (p=0.015) and PR-positive BC patients (p=0.018) than in DCIS patients. Exosomal miR-16 could differ between ER-positive and -negative (p=0.004). As well as between PR-positive and -negative (p=0.008) BC patients. Triple-negative patients had lower levels of miR-16 than the receptor-positive patients (p=0.012, Table 3.3), specifically, than ER-positive BC patients (p=0.009) and PR-positive BC patients (p=0.010). These findings show that the increased levels of miR-16 in exosomes from recurrent BC patients decreased in receptor-negative patients. Moreover, the levels of exosomal miR-30b and miR-93 could distinguish lobular/tubular BC from other histological subtypes (p=0.024) and PR-positive from -negative BC (p=0.010), respectively (Table 3.3). The levels of exosomal miR-93 were higher in ER-positive BC patients (p=0.033) and PR-positive BC patients (p=0.015) than in healthy women. They were also higher in DCIS patients than in ER-negative BC patients (p=0.003), PR-negative BC patients (p=0.0001) and triple-negative patients (p=0.007, Figure 3.13.C).

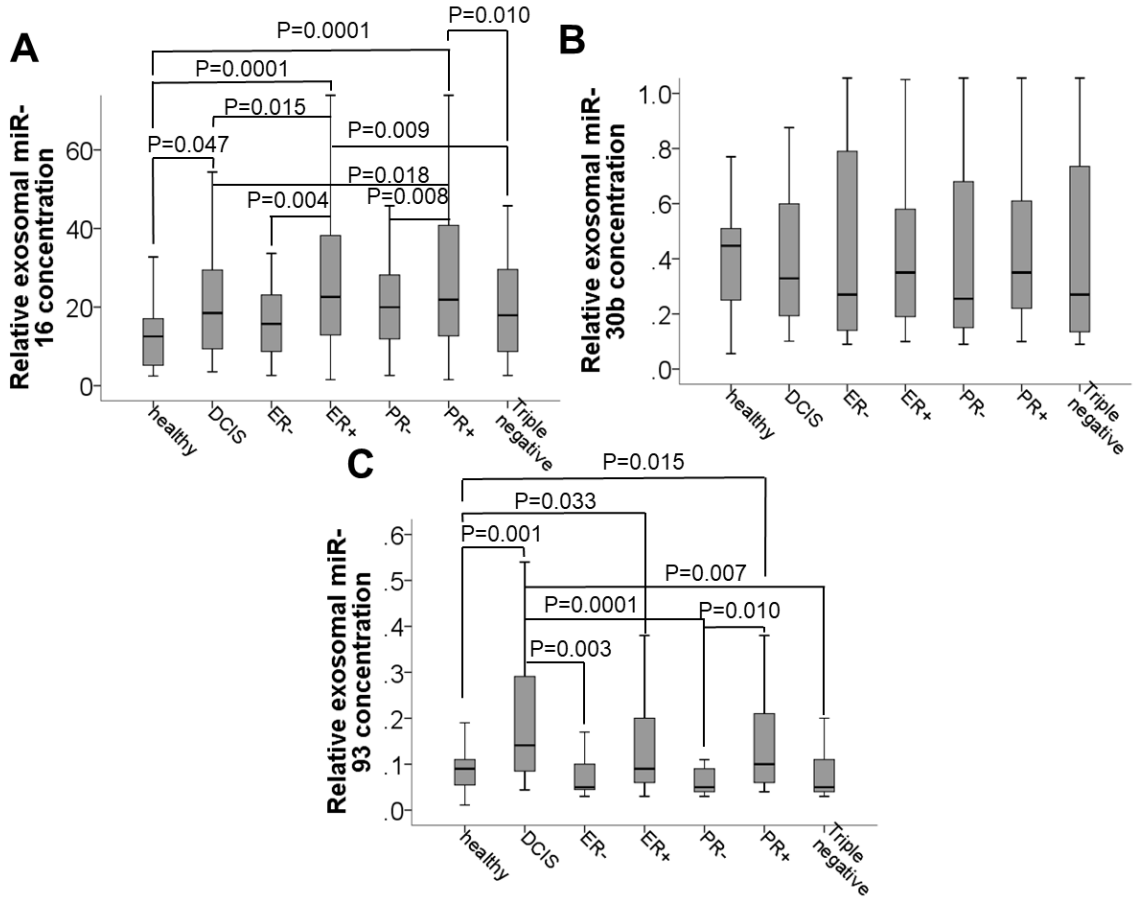

Figure 3.13. Deregulated levels of exosomal miR-16, miR-30b and miR-93 in DCIS patients and BC patient subgroups

The 3 box blots show the plasma levels of exosomal miR-16 (A), miR-30b (B) and miR-93 (C) in 39 healthy women, 42 DCIS patients and 109 BC patients.

28 ER-negative, 81 ER-positive; 35 PR-negative, 74 PR-positive; 24 triple-negative.

P-values are indicated.

4. Discussion

4.1. Investigations of the effects by EMFs on BC cell lines

The aim of this part of my study was to find a specific frequency of EMF which has an inhibitory effect on cell growth, exosome release, and DNA hypermethylation, as well as a stimulation effect on DNA hydroxymethylation in MCF-7, MDA-MB-231 and MDA-MB-468 cells, but no impact on normal MCF-10A cells. Experiment II with the frequency of 73 Hz and experiment VIII with a frequency of 31 Hz showed the best result. Therefore, I repeated these experiments 3 times.

In experiment II and VIII an increase in cell numbers was observed in all BC cell lines except MDA-MB-468 in comparison with normal cell MCF-10A. However, the aim of the study was to decrease the cell number. It was reported that EMF [a 3 ms interval for the first 5 repeats (25 Hz) to a 120 ms interval (6 Hz) for the last 5 repeats] inhibited the growth of MDA-MB-231 and MCF-7 but did not affect the growth of non-malignant cells (38). The different results may be explained by the use of different frequencies of EMFs.

Changes in DNA methylation are a common early event in carcinogenesis. During transformation of a benign to a malignant cell a global DNA hypomethylation with a region-specific hypermethylation on tumor suppressor gene occurs. Previously it was shown that 900 MHz EMF exposure can affect the alterations of genome-wide methylation (91). In experiment II and VIII, EMF had no impact on 5-mC DNA in all cell lines, suggesting that exposure time and strength of EMFs were insufficient.

It was reported that reduction of global 5-hmC is a poor prognostic factor in BC patients (92), and that 5-hmC may play an important role in oncogenesis (93). In experiment II and VIII the highest stimulatory effect was on MDA-MB-468 in comparison with normal MCF-10A cells, suggesting an efficient hydroxylation of DNA.

It was reported that increased secretion of exosomes has been associated with tumor invasiveness (71, 94). In experiment II and VIII an increase in the levels of exosome was observed in normal MCF-10A cells, thus contrary non-expected effect.

In summary, I found that there were no big, but versatile changes in exosome release, cell number and DNA methylation in BC cells by applying different frequencies of EMF. Only the changes in DNA hydroxymethylation were relatively stable and promising. However, there were intra-assay and inter-assay differences. Further experiments need to be done to prolong the exposure time and apply further frequencies.

4.2. Circulating exosomal microRNAs in blood of BC patients

In the present study I analyzed the signature of miR-16, miR-30b and miR-93 in exosomes derived from plasma of BC patients and compared it with that in DCIS patients and healthy women using quantitative TaqMan real-time PCR-based microarray cards and single PCR assays. I found that the data derived from these both techniques were only partly overlapping, suggesting that the number of patients and healthy women was too low in the array assays to get robust p-values. It is rather unlikely that the difference in data is caused by the use of two different techniques because the tendency of the deregulation of these three miRNAs is similar. In particular, the significant enrichment of miR-93 in exosomes from DCIS patients compared with healthy women and BC patients was detected by both techniques. Although my patient cohorts are small and further analyses are necessary, my findings point to an association of exosomal miR-93 with DCIS. Approximately one of five breast tumors detected by mammography is diagnosed as DCIS (95). But it is still challenging to distinguish DCIS cases that are likely to progress from cases that remain indolent, and therefore do not require intensive treatment. In this regard, Lesurf et al. established a specific signature able to identify pre-invasive DCIS harboring a miRNA expression profile that resembles invasive carcinoma, indicating that these DCIS cases have a higher likelihood of future disease progression (96). Concerning miR-93, further follow-up analyses are necessary to determine whether the enrichment of this miRNA in exosomes also reflects a possible future invasiveness of DCIS. Particularly, considering the high cancer-specific secretion of exosomes that are important mediators between tumor and its

microenvironment, the exosome shuttle of miR-93 could contribute to increase cell invasion (97). By the way, it was reported that upregulation of miR-93 promoted cell migration, invasion and proliferation in BC, as well as participated in regulating angiogenesis in cancers (98-100). Moreover, PTEN (Phosphatase Tensin Homolog) seems to be a target of miR-93, and consequently, miR-93 may regulate the activity of PI3K/Akt (Phosphoinositide 3-kinase/ Protein Kinase B) pathway (98). Previously, we observed higher transcript concentrations of circulating miR-93 in primary BC patients than in healthy women, but not in BC patient with metastasis (90). However, in the present study the enrichment of miR-93 in exosomes from BC patients was only of borderline significance. To date, I only found one article that quantified miR-93 in exosomes from BC patients. This study by Sueta et al. showed that the levels of miR-93 in tumor tissues was upregulated, but downregulated in exosomes from serum of patients with recurrence compared with those with no recurrence (101). I did not observe such an association of exosomal miR-93 with recurrence. This discrepancy could be explained by the small cohort used in that study that quantified exosomal miR-93, in only 16 recurrent and 16 non-recurrent BC patients. Furthermore, Kolacinska et al. found that the levels of miR-93 were higher in biopsy cells from ER- and PR-negative BC patients than from ER- and PR-positive BC (102). In contrast, I observed lower levels of exosomal miR-93 in PR-negative BC patients than in PR-positive BC. The different results may be explained by the specific packaging of miRNAs in exosomes. I also detected that the levels of exosomal miR-93 were lower in ER-, PR- and triple-negative BC patients than in DCIS patients, whereas ER- and PR-positive BC patients had higher levels of this miRNA than healthy women. Nonetheless, these data demonstrate differently deregulated levels of miRNAs between exosomes and tumor tissues, and a selective packaging process of miRNAs into exosomes that is not related to their expression levels in the primary tumor.

Discrepant data on miR-16 exist in numerous publications that describe this miRNA as tumor suppressor gene, oncogene or reference miRNA (80, 103, 104). My findings show that the enrichment of miR-16 in exosomes is especially associated with recurrence and receptor status. I found higher levels of exosomal miR-16 in ER- and PR-positive BC patients than in

healthy women, DCIS patients, ER-, PR- and triple-negative BC patients, as well as higher levels in BC patients with recurrence than in healthy women and DCIS patients. These findings suggest a selective and wavelike packaging of miR-16 into exosomes in the different subtypes, and possibly during tumor development and progression. Chernyi et al. also detected a higher expression of miR-16 in ER-positive tumors (105). As far as I know there are no study that quantified miR-16 in exosomes from BC patients. To date, our previous data show that the increased plasma levels of miR-16 in BC patients compared with healthy women were associated with lymph node status, but they did not provide any indication of an association with the receptor status (87), indicating, again that higher levels of miR-16 in plasma do not implicate a higher enrichment in exosomes.

Finally, I detected no deregulated levels of miR-30b in exosomes from BC patients, but the levels of exosomal miR-30b could differ between primary and recurrent BC, as well as between lobular/tubular and other histological BC. Interestingly, a study by Tormo et al. showed that miR-30b may regulate trastuzumab resistance and Cyclin E2 gene in HER2-positive BC patients (106). Similarly, trastuzumab inhibit BC cell growth by upregulating miR-30b (107).

In conclusion, my findings show a specific packaging of miR-16, miR-30b and miR-93 into exosomes from BC and DCIS patients. In particular, miR-93 was significantly enriched in exosomes from DCIS patients. Further follow-up studies are needed to investigate whether exosomal secretion of miR-93 may impact signaling in nearby breast cells and stimulate their invasiveness.

5. Summary

The aim of the first part of my study was to find a specific frequency of EMF which has an inhibitory effect on cell growth, exosome release, DNA hypermethylation and a stimulatory effect on DNA hydroxymethylation in MCF-7, MDA-MB-231 and MDA-MB-468 cells, but no impact on normal MCF-10A cells. In summary, I found that there were no big, but versatile changes in exosome release, cell number and DNA methylation in BC cells by applying different frequencies of EMF. Only the increase in DNA hydroxymethylation was relatively stable and promising. Further experiments need to be done to prolong the exposure time and apply further frequencies.

Specific packaging of miRNAs in exosomes promotes tumor development and progression. In my study, I analyzed the signature of miR-16, miR-30b and miR-93 in exosomes derived from plasma of BC patients and compared it with that in DCIS patients and healthy women using quantitative TaqMan real-time PCR-based microarray cards and single PCR assays. I carried out the microarray with cards containing 45 different miRNAs (plus 3 references), to determine the miRNA expression profiles in exosomes derived from the plasma of 32 BC (16 primary and 16 recurrent) patients, 8 DCIS patients and 8 healthy women. Then, 3 significantly deregulated exosomal miRNAs (miR-16, miR-30b and miR-93) derived from these array analyses were selected for single TaqMan real-time PCR assays using exosomes from plasma of 111 BC patients, 42 DCIS patients and 39 healthy women. Identification of exosomes was performed by Western blot. In conclusion, my findings show a specific packaging of miR-16, miR-30b and miR-93 into exosomes from BC and DCIS patients. In particular, the levels of exosomal miR-16 were different in the various BC subtypes. MiR-93 was significantly enriched in exosomes from DCIS patients. Further follow-up studies are needed to investigate whether exosomal secretion of miR-93 may impact signaling in nearby breast cells and stimulate their invasiveness.

Zusammenfassung

Das Ziel des ersten Teils meiner Studie war es, eine spezifische Frequenz für EMF zu finden, die eine inhibierende Wirkung auf Zellwachstum, Freisetzung von Exosomen, DNA-Hypermethylierung und eine stimulierende Wirkung auf DNA-Hydroxymethylierung in MCF-7, MDA-MB-231 und MDA-MB-468-Zellen hat, aber keine Wirkung auf normale MCF-10A-Zellen. Zusammenfassend fand ich, dass es kaum, aber vielseitigen Veränderungen in der Freisetzung von Exosomen, Zellzahl und DNA-Methylierung in BC-Zellen durch Anwenden verschiedener EMF-Frequenzen gab. Nur der Anstieg der DNA-Hydroxymethylierung war relativ stabil und vielversprechend. Weitere Experimente müssen durchgeführt werden, um die Expositionsszeit zu verlängern und weitere Frequenzen anzuwenden.

Die spezifische Verpackung von miRNAs in Exosomen fördert die Tumorentwicklung und Progression. In meiner Studie analysierte ich die Signatur von miR-16, miR-30b und miR-93 in Exosomen aus Plasma von BC-Patientinnen und verglich sie mit denen von DCIS-Patientinnen und gesunden Frauen, indem ich quantitative TaqMan real-time PCR-basierte Microarrays und einzelne PCR-Assays durchführte. Ich führte den Microarray mit Karten von 45 verschiedenen miRNAs (plus 3 Referenzen) durch, um die miRNA Expressionsprofile in Exosomen aus dem Plasma von 32 BC (16 primäre und 16 rezidivierende) Patientinnen, 8 DCIS Patientinnen und 8 gesunde Frauen zu bestimmen. Dann wurden 3 signifikant deregulierte exosomale miRNAs (miR-16, miR-30b und miR-93), aufgrund dieser Array-Analysen, für die einzelnen TaqMan-Real-Time-PCR-Assays unter Verwendung von Exosomen aus Plasma von 111 BC-Patientinnen, 42 DCIS-Patientinnen und 39 gesunden Frauen ausgewählt. Die Identifizierung von Exosomen erfolgte durch Western Blot. Zusammenfassend zeigen meine Ergebnisse eine spezifische Verpackung von miR-16, miR-30b und miR-93 in Exosomen von BC- und DCIS-Patientinnen. Insbesondere waren die Spiegel der exosomalen miR-16 in den verschiedenen BC-Subtypen unterschiedlich. MiR-93 wurde signifikant in Exosomen von DCIS-Patientinnen angereichert. Weitere Untersuchungen sind erforderlich, um zu zeigen, ob die exosomale Sekretion von miR-93 die Signalgebung in benachbarten Brustzellen beeinflusst und deren Invasivität stimuliert.

6. List of abbreviations

%	Percent
°C	Celsius Degree
5-hmC	5-hydroxymethylcytosine
5-mC	5-methylcytosine
AGO2	Argonaute-2
AJCC	American Joint Committee on Cancer
AKT	Protein Kinase B
ATCC	American Type Culture Collection
BC	Breast Cancer
BRCA1	Breast Cancer, early onset 1
BRCA2	Breast Cancer, early onset 2
BSA	Bovine Serum Albumin
cDNA	Complementary DNA
CIT	Cell Information Therapy
CO_2	Carbon Dioxide
CpG	Cytosine-phosphate-guanine
Cq	Cycle of Quantification
DCIS	Ductal carcinoma in situ
DNMT	DNA methyltransferases
EDTA	Ethylenediaminetetraacetic acid
ELF	Extremely low frequency
ELISA	Enzyme-linked immunosorbent assay
EMF	Electromagnetic field
EMT	Epithelial-mesenchymal transition
ER	Estrogen receptor
et al.	etalii/etaliae
FBS	Fetal Bovine Serum
FCS	Fetal Calf Serum
g	Gram
g	Gravity
G	Grading
h	Hour
H_2O_2	Hydrogen Peroxide
HCl	Hydrochloric Acid
HER2	human epidermal growth factor 2

HRP	Horseradish Peroxidase
Hz	Hertz
kDa	Kilodalton
l	Liter
mAb	monoclonal antibody
MAP	Mitogen-activated protein
MET	Mesenchymal-epithelial transition
mg	Milligram
$MgCl_2$	Magnesium chloride
MHz	Million hertz
min	Minute
miR	MicroRNA
miRNAs	MicroRNAs
ml	Milliliter
mm	Millimetre
mM	Millimole
MRI	Magnetic resonance imaging
mRNA	Messenger Ribonucleic Acid
ms	Millisecond
mT	Millitesla
MVBs	Multivesicular Bodies
NCI-NIH	National Cancer Institute-National Institute of Health
ncRNAs	Non-coding RNAs
ng	Nanogram
nm	Nanometer
nM	Nanomole
NST	Non-special type
OD	Optical Density
ORF	Open Reading Frame
pAb	Polyclonal Antibody
PBS	Phosphate Buffered Saline
PCR	Polymerase Chain Reaction
pH	Hydrogen Ion Concentration
PI3K	Phosphoinositide 3-kinase
pre-miR	Precursor microRNA
pri-miR	Primary microRNA
PR	Progesterone receptor

PTEN	Phosphatase Tensin Homolog
PVDF	Polyvinylidene Fluoride
PCR	Polymerase Chain Reaction
qPCR	Quantitative Polymerase Chain Reaction
RISC	RNA-Induced Silencing Complex
RNase	Ribonuclease
rpm	Revolutions Per Minute
RT	Reverse Transcription
RT	Room Temperature
SBR	Scarff-Bloom-Richardson
SDS-PAGE	Sodium Dodecyl Sulfate-Polyacrylamide Gel Electrophoresis
sec	Second
SPSS	Statistical Product and Service Solutions
TBST	Tris-Buffered Saline Tween
TE	Tris-EDTA
TET	Ten-eleven translocation proteins
Tris	Tris(hydroxymethyl)aminomethane
U	Unit
UTR	Untranslated Region
V	Voltage
µg	Microgram
µl	Microliter
µm	Micrometer

7. Reference

1. Ferlay J, Soerjomataram I, Dikshit R, Eser S, Mathers C, Rebelo M, et al. Cancer incidence and mortality worldwide: sources, methods and major patterns in GLOBOCAN 2012. Int J Cancer. 2015;136(5):E359-86.

2. American cancer society [Available from: https://www.cancer.org/cancer/breast-cancer/about/how-common-is-breast-cancer.html.

3. McGuire A, Brown JA, Kerin MJ. Metastatic breast cancer: the potential of miRNA for diagnosis and treatment monitoring. Cancer Metastasis Rev. 2015;34(1):145-55.

4. Bodai BI, Tuso P. Breast cancer survivorship: a comprehensive review of long-term medical issues and lifestyle recommendations. Perm J. 2015;19(2):48-79.

5. Donepudi MS, Kondapalli K, Amos SJ, Venkanteshan P. Breast cancer statistics and markers. J Cancer Res Ther. 2014;10(3):506-11.

6. Sanford SD, Zhao F, Salsman JM, Chang VT, Wagner LI, Fisch MJ. Symptom burden among young adults with breast or colorectal cancer. Cancer. 2014;120(15):2255-63.

7. Collaborative Group on Hormonal Factors in Breast C. Familial breast cancer: collaborative reanalysis of individual data from 52 epidemiological studies including 58,209 women with breast cancer and 101,986 women without the disease. Lancet. 2001;358(9291):1389-99.

8. Autier P. Risk factors for breast cancer for women aged 40 to 49 years. Ann Intern Med. 2012;157(7):529; author reply

9. Minatoya M, Kutomi G, Asakura S, Otokozawa S, Sugiyama Y, Nagata Y, et al. Equol, adiponectin, insulin levels and risk of breast cancer. Asian Pac J Cancer Prev. 2013;14(4):2191-9.

10. Tice JA, Cummings SR, Smith-Bindman R, Ichikawa L, Barlow WE, Kerlikowske K. Using clinical factors and mammographic breast density to estimate breast cancer risk: development and validation of a new predictive model. Ann Intern Med. 2008;148(5):337-47.

11. Howell A, Anderson AS, Clarke RB, Duffy SW, Evans DG, Garcia-Closas M, et al. Risk determination and prevention of breast cancer. Breast Cancer Res. 2014;16(5):446.

12. Westbrook K, Stearns V. Pharmacogenomics of breast cancer therapy: an update. Pharmacol Ther. 2013;139(1):1-11.

13. Broeders M, Moss S, Nystrom L, Njor S, Jonsson H, Paap E, et al. The impact of mammographic screening on breast cancer mortality in Europe: a review of observational studies. J Med Screen. 2012;19 Suppl 1:14-25.

14. Hofvind S, Ursin G, Tretli S, Sebuodegard S, Moller B. Breast cancer mortality in participants of the Norwegian Breast Cancer Screening Program. Cancer. 2013;119(17):3106-12.

15. Youl PH, Aitken JF, Turrell G, Chambers SK, Dunn J, Pyke C, et al. The Impact of Rurality and Disadvantage on the Diagnostic Interval for Breast Cancer in a Large Population-Based Study of 3202 Women in Queensland, Australia. Int J Env Res Pub He. 2016;13(11).

16. Chand AR, Ziauddin MF, Tang SC. Can Locoregionally Recurrent Breast Cancer Be Cured? Clin Breast Cancer. 2017;17(5):326-35.

17. Dai X, Li T, Bai Z, Yang Y, Liu X, Zhan J, et al. Breast cancer intrinsic subtype classification, clinical use and future trends. Am J Cancer Res. 2015;5(10):2929-43.

18. Hennigs A, Riedel F, Gondos A, Sinn P, Schirmacher P, Marme F, et al. Prognosis of breast cancer molecular subtypes in routine clinical care: A large prospective cohort study. BMC Cancer. 2016;16(1):734.

19. Tai W, Mahato R, Cheng K. The role of HER2 in cancer therapy and targeted drug delivery. J Control Release. 2010;146(3):264-75.

20. Bansal C, Pujani M, Sharma KL, Srivastava AN, Singh US. Grading systems in the cytological diagnosis of breast cancer: a review. J Cancer Res Ther. 2014;10(4):839-45.

21. McCart Reed AE, Kutasovic JR, Lakhani SR, Simpson PT. Invasive lobular carcinoma of the breast: morphology, biomarkers and 'omics. Breast Cancer Res. 2015;17:12.

22. Rakha EA, Lee AH, Evans AJ, Menon S, Assad NY, Hodi Z, et al. Tubular carcinoma of the breast: further evidence to support its excellent prognosis. J Clin Oncol. 2010;28(1):99-104.

23. Sherman ME, Mies C, Gierach GL. Opportunities for molecular epidemiological research on ductal carcinoma in-situ and breast carcinogenesis: interdisciplinary approaches. Breast Dis. 2014;34(3):105-16.

24. Ross DS, Wen YH, Brogi E. Ductal carcinoma in situ: morphology-based knowledge and molecular advances. Adv Anat Pathol. 2013;20(4):205-16.

25. Leonard GD, Swain SM. Ductal carcinoma in situ, complexities and challenges. J Natl Cancer Inst. 2004;96(12):906-20.

26. Kuerer HM, Albarracin CT, Yang WT, Cardiff RD, Brewster AM, Symmans WF, et al. Ductal carcinoma in situ: state of the science and roadmap to advance the field. J Clin Oncol. 2009;27(2):279-88.

27. Siegel R, Ma J, Zou Z, Jemal A. Cancer statistics, 2014. CA Cancer J Clin. 2014;64(1):9-29.

28. Siziopikou KP. Ductal carcinoma in situ of the breast: current concepts and future directions. Arch Pathol Lab Med. 2013;137(4):462-6.

29. Yu KD, Wu LM, Liu GY, Wu J, Di GH, Shen ZZ, et al. Different distribution of breast cancer subtypes in breast ductal carcinoma in situ (DCIS), DCIS with microinvasion, and DCIS with invasion component. Ann Surg Oncol. 2011;18(5):1342-8.

30. Richards T, Hunt A, Courtney S, Umeh H. Nipple discharge: a sign of breast cancer? Ann R Coll Surg Engl. 2007;89(2):124-6.

31. Mitchell KB, Kuerer H. Ductal Carcinoma In Situ: Treatment Update and Current Trends. Curr Oncol Rep. 2015;17(11):48.

32. Sackey H, Hui M, Czene K, Verkooijen H, Edgren G, Frisell J, et al. The impact of in situ breast cancer and family history on risk of subsequent breast cancer events and mortality - a population-based study from Sweden. Breast Cancer Res. 2016;18(1):105.

33. Early Breast Cancer Trialists' Collaborative G, Correa C, McGale P, Taylor C, Wang Y, Clarke M, et al. Overview of the randomized trials of radiotherapy in ductal carcinoma in situ of the breast. J Natl Cancer Inst Monogr. 2010;2010(41):162-77.

34. Williams KE, Barnes NLP, Cramer A, Johnson R, Cheema K, Morris J, et al. Molecular phenotypes of DCIS predict overall and invasive recurrence. Ann Oncol. 2015;26(5):1019-25.

35. Lewczuk B, Redlarski G, Zak A, Ziolkowska N, Przybylska-Gornowicz B, Krawczuk M. Influence of electric, magnetic, and electromagnetic fields on the circadian system: current stage of knowledge. Biomed Res Int. 2014;2014:169459.

36. Ehnert S, Fentz AK, Schreiner A, Birk J, Wilbrand B, Ziegler P, et al. Extremely low frequency pulsed electromagnetic fields cause antioxidative defense mechanisms in human osteoblasts via induction of *O2(-) and H2O2. Sci Rep. 2017;7(1):14544.

37. Bassett CA. Beneficial effects of electromagnetic fields. J Cell Biochem. 1993;51(4):387-93.

38. Buckner CA, Buckner AL, Koren SA, Persinger MA, Lafrenie RM. Inhibition of cancer cell growth by exposure to a specific time-varying electromagnetic field involves T-type calcium channels. PLoS One. 2015;10(4):e0124136.

39. Buckner CA, Buckner AL, Koren SA, Persinger MA, Lafrenie RM. Exposure to a specific time-varying electromagnetic field inhibits cell proliferation via cAMP and ERK signaling in cancer cells. Bioelectromagnetics. 2017.

40. Zhang X, Liu X, Pan L, Lee I. Magnetic fields at extremely low-frequency (50 Hz, 0.8 mT) can induce the uptake of intracellular calcium levels in osteoblasts. Biochem Biophys Res Commun. 2010;396(3):662-6.

41. Koziorowska A, Pasiud E, Fila M, Romerowicz-Misielak M. THE IMPACT OF ELECTROMAGNETIC FIELD AT A FREQUENCY OF 50 HZ AND A MAGNETIC INDUCTION OF 2.5 mT ON VIABILITY OF PINEAL CELLS IN VITRO. J Biol Reg Homeos Ag. 2016;30(4):1067-72.

42. Kang KS, Hong JM, Seol YJ, Rhie JW, Jeong YH, Cho DW. Short-term evaluation of electromagnetic field pretreatment of adipose-derived stem cells to improve bone healing. J Tissue Eng Regen Med. 2015;9(10):1161-71.

43. Ryang We S, Koog YH, Jeong KI, Wi H. Effects of pulsed electromagnetic field on knee osteoarthritis: a systematic review. Rheumatology (Oxford). 2013;52(5):815-24.

44. Mahmoudinasab H, Sanie-Jahromi F, Saadat M. Effects of extremely low-frequency electromagnetic field on expression levels of some antioxidant genes in MCF-7 cells. Mol Biol Res Commun. 2016;5(2):77-85.

45. Crocetti S, Beyer C, Schade G, Egli M, Frohlich J, Franco-Obregon A. Low intensity and frequency pulsed electromagnetic fields selectively impair breast cancer cell viability. PLoS One. 2013;8(9):e72944.

46. Buckner CA, Buckner AL, Koren SA, Persinger MA, Lafrenie RM. The effects of electromagnetic fields on B16-BL6 cells are dependent on their spatial and temporal character. Bioelectromagnetics. 2017;38(3):165-74.

47. Guerrero-Preston R, Baez A, Blanco A, Berdasco M, Fraga M, Esteller M. Global DNA methylation: a common early event in oral cancer cases with exposure to environmental carcinogens or viral agents. P R Health Sci J. 2009;28(1):24-9.

48. Chen CC, Wang KY, Shen CK. DNA 5-methylcytosine demethylation activities of the mammalian DNA methyltransferases. J Biol Chem. 2013;288(13):9084-91.

49. Deaton AM, Bird A. CpG islands and the regulation of transcription. Genes Dev. 2011;25(10):1010-22.

50. Smith ZD, Meissner A. DNA methylation: roles in mammalian development. Nat Rev Genet. 2013;14(3):204-20.

51. Moore LD, Le T, Fan G. DNA methylation and its basic function. Neuropsychopharmacology. 2013;38(1):23-38.

52. Bird A. DNA methylation patterns and epigenetic memory. Genes Dev. 2002;16(1):6-21.

53. Jeltsch A, Jurkowska RZ. New concepts in DNA methylation. Trends Biochem Sci. 2014;39(7):310-8.

54. Kriaucionis S, Heintz N. The nuclear DNA base 5-hydroxymethylcytosine is present in Purkinje neurons and the brain. Science. 2009;324(5929):929-30.

55. Tahiliani M, Koh KP, Shen Y, Pastor WA, Bandukwala H, Brudno Y, et al. Conversion of 5-methylcytosine to 5-hydroxymethylcytosine in mammalian DNA by MLL partner TET1. Science. 2009;324(5929):930-5.

56. Pastor WA, Aravind L, Rao A. TETonic shift: biological roles of TET proteins in DNA demethylation and transcription. Nat Rev Mol Cell Biol. 2013;14(6):341-56.

57. Li W, Liu M. Distribution of 5-hydroxymethylcytosine in different human tissues. J Nucleic Acids. 2011;2011:870726.

58. Harding C, Heuser J, Stahl P. Receptor-mediated endocytosis of transferrin and recycling of the transferrin receptor in rat reticulocytes. J Cell Biol. 1983;97(2):329-39.

59. Pan BT, Johnstone RM. Fate of the transferrin receptor during maturation of sheep reticulocytes in vitro: selective externalization of the receptor. Cell. 1983;33(3):967-78.

60. Horibe S, Tanahashi T, Kawauchi S, Murakami Y, Rikitake Y. Mechanism of recipient cell-dependent differences in exosome uptake. BMC Cancer. 2018;18(1):47.

61. Thery C, Zitvogel L, Amigorena S. Exosomes: composition, biogenesis and function. Nat Rev Immunol. 2002;2(8):569-79.

62. Hessvik NP, Llorente A. Current knowledge on exosome biogenesis and release. Cell Mol Life Sci. 2018;75(2):193-208.

63. Mathivanan S, Simpson RJ. ExoCarta: A compendium of exosomal proteins and RNA. Proteomics. 2009;9(21):4997-5000.

64. Kahlert C, Kalluri R. Exosomes in tumor microenvironment influence cancer progression and metastasis. J Mol Med (Berl). 2013;91(4):431-7.

65. M HR, Bayraktar E, G KH, Abd-Ellah MF, Amero P, Chavez-Reyes A, et al. Exosomes: From Garbage Bins to Promising Therapeutic Targets. Int J Mol Sci. 2017;18(3).

66. Schwarzenbach H. The clinical relevance of circulating, exosomal miRNAs as biomarkers for cancer. Expert Rev Mol Diagn. 2015;15(9):1159-69.

67. Thery C. Exosomes: secreted vesicles and intercellular communications. F1000 Biol Rep. 2011;3:15.

68. Qin J, Xu Q. Functions and application of exosomes. Acta Pol Pharm. 2014;71(4):537-43.

69. Hood JL, Wickline SA. A systematic approach to exosome-based translational nanomedicine. Wiley Interdiscip Rev Nanomed Nanobiotechnol. 2012;4(4):458-67.

70. Milane L, Singh A, Mattheolabakis G, Suresh M, Amiji MM. Exosome mediated communication within the tumor microenvironment. J Control Release. 2015;219:278-94.

71. Azmi AS, Bao B, Sarkar FH. Exosomes in cancer development, metastasis, and drug resistance: a comprehensive review. Cancer Metastasis Rev. 2013;32(3-4):623-42.

72. Eichelser C, Stuckrath I, Muller V, Milde-Langosch K, Wikman H, Pantel K, et al. Increased serum levels of circulating exosomal microRNA-373 in receptor-negative breast cancer patients. Oncotarget. 2014;5(20):9650-63.

73. Meng X, Muller V, Milde-Langosch K, Trillsch F, Pantel K, Schwarzenbach H. Diagnostic and prognostic relevance of circulating exosomal miR-373, miR-200a, miR-200b and miR-200c in patients with epithelial ovarian cancer. Oncotarget. 2016;7(13):16923-35.

74. Greening DW, Gopal SK, Xu R, Simpson RJ, Chen W. Exosomes and their roles in immune regulation and cancer. Semin Cell Dev Biol. 2015;40:72-81.

75. Hood JL, San RS, Wickline SA. Exosomes released by melanoma cells prepare sentinel lymph nodes for tumor metastasis. Cancer Res. 2011;71(11):3792-801.

76. O'Brien K, Rani S, Corcoran C, Wallace R, Hughes L, Friel AM, et al. Exosomes from triple-negative breast cancer cells can transfer phenotypic traits representing their cells of origin to secondary cells. Eur J Cancer. 2013;49(8):1845-59.

77. Batrakova EV, Kim MS. Using exosomes, naturally-equipped nanocarriers, for drug delivery. J Control Release. 2015;219:396-405.

78. Osaki M, Okada F, Ochiya T. miRNA therapy targeting cancer stem cells: a new paradigm for cancer treatment and prevention of tumor recurrence. Ther Deliv. 2015;6(3):323-37.

79. Krol J, Loedige I, Filipowicz W. The widespread regulation of microRNA biogenesis, function and decay. Nat Rev Genet. 2010;11(9):597-610.

80. Schwarzenbach H, Nishida N, Calin GA, Pantel K. Clinical relevance of circulating cell-free microRNAs in cancer. Nat Rev Clin Oncol. 2014;11(3):145-56.

81. Chen X. MicroRNA biogenesis and function in plants. FEBS Lett. 2005;579(26):5923-31.

82. Calin GA, Dumitru CD, Shimizu M, Bichi R, Zupo S, Noch E, et al. Frequent deletions and down-regulation of micro- RNA genes miR15 and miR16 at 13q14 in chronic lymphocytic leukemia. Proc Natl Acad Sci U S A. 2002;99(24):15524-9.

83. Di Leva G, Garofalo M, Croce CM. MicroRNAs in cancer. Annu Rev Pathol. 2014;9:287-314.

84. Cheng AM, Byrom MW, Shelton J, Ford LP. Antisense inhibition of human miRNAs and indications for an involvement of miRNA in cell growth and apoptosis. Nucleic Acids Res. 2005;33(4):1290-7.

85. Pant S, Hilton H, Burczynski ME. The multifaceted exosome: biogenesis, role in normal and aberrant cellular function, and frontiers for pharmacological and biomarker opportunities. Biochem Pharmacol. 2012;83(11):1484-94.

86. Shelke GV, Lasser C, Gho YS, Lotvall J. Importance of exosome depletion protocols to eliminate functional and RNA-containing extracellular vesicles from fetal bovine serum. J Extracell Vesicles. 2014;3.

87. Stuckrath I, Rack B, Janni W, Jager B, Pantel K, Schwarzenbach H. Aberrant plasma levels of circulating miR-16, miR-107, miR-130a and miR-146a are associated with lymph node metastasis and receptor status of breast cancer patients. Oncotarget. 2015;6(15):13387-401.

88. Joosse SA, Muller V, Steinbach B, Pantel K, Schwarzenbach H. Circulating cell-free cancer-testis MAGE-A RNA, BORIS RNA, let-7b and miR-202 in the blood of patients with breast cancer and benign breast diseases. Br J Cancer. 2014;111(5):909-17.

89. Muller V, Gade S, Steinbach B, Loibl S, von Minckwitz G, Untch M, et al. Changes in serum levels of miR-21, miR-210, and miR-373 in HER2-positive breast cancer patients undergoing neoadjuvant therapy: a translational research project within the Geparquinto trial. Breast Cancer Res Treat. 2014;147(1):61-8.

90. Eichelser C, Flesch-Janys D, Chang-Claude J, Pantel K, Schwarzenbach H. Deregulated serum concentrations of circulating cell-free microRNAs miR-17, miR-34a, miR-155, and miR-373 in human breast cancer development and progression. Clin Chem. 2013;59(10):1489-96.

91. Mokarram P, Sheikhi M, Mortazavi SMJ, Saeb S, Shokrpour N. Effect of Exposure to 900 MHz GSM Mobile Phone Radiofrequency Radiation on Estrogen Receptor Methylation Status in Colon Cells of Male Sprague Dawley Rats. J Biomed Phys Eng. 2017;7(1):79-86.

92. Tsai KW, Li GC, Chen CH, Yeh MH, Huang JS, Tseng HH, et al. Reduction of global 5-hydroxymethylcytosine is a poor prognostic factor in breast cancer patients, especially for an ER/PR-negative subtype. Breast Cancer Res Treat. 2015;153(1):219-34.

93. Zhang LY, Li PL, Wang TZ, Zhang XC. Prognostic values of 5-hmC, 5-mC and TET2 in epithelial ovarian cancer. Arch Gynecol Obstet. 2015;292(4):891-7.

94. Jenjaroenpun P, Kremenska Y, Nair VM, Kremenskoy M, Joseph B, Kurochkin IV. Characterization of RNA in exosomes secreted by human breast cancer cell lines using next-generation sequencing. PeerJ. 2013;1:e201.

95. Gorringe KL, Fox SB. Ductal Carcinoma In Situ Biology, Biomarkers, and Diagnosis. Front Oncol. 2017;7:248.

96. Lesurf R, Aure MR, Mork HH, Vitelli V, Oslo Breast Cancer Research C, Lundgren S, et al. Molecular Features of Subtype-Specific Progression from Ductal Carcinoma In Situ to Invasive Breast Cancer. Cell Rep. 2016;16(4):1166-79.

97. Steinbichler TB, Dudas J, Riechelmann H, Skvortsova, II. The role of exosomes in cancer metastasis. Semin Cancer Biol. 2017;44:170-81.

98. Li N, Miao Y, Shan Y, Liu B, Li Y, Zhao L, et al. MiR-106b and miR-93 regulate cell progression by suppression of PTEN via PI3K/Akt pathway in breast cancer. Cell Death Dis. 2017;8(5):e2796.

99. Liang L, Zhao L, Zan Y, Zhu Q, Ren J, Zhao X. MiR-93-5p enhances growth and angiogenesis capacity of HUVECs by down-regulating EPLIN. Oncotarget. 2017;8(63):107033-43.

100. Fang L, Deng Z, Shatseva T, Yang J, Peng C, Du WW, et al. MicroRNA miR-93 promotes tumor growth and angiogenesis by targeting integrin-beta8. Oncogene. 2011;30(7):806-21.

101. Sueta A, Yamamoto Y, Tomiguchi M, Takeshita T, Yamamoto-Ibusuki M, Iwase H. Differential expression of exosomal miRNAs between breast cancer patients with and without recurrence. Oncotarget. 2017;8(41):69934-44.

102. Kolacinska A, Morawiec J, Pawlowska Z, Szemraj J, Szymanska B, Malachowska B, et al. Association of microRNA-93, 190, 200b and receptor status in core biopsies from stage III breast cancer patients. DNA Cell Biol. 2014;33(9):624-9.

103. Schwarzenbach H, da Silva AM, Calin G, Pantel K. Data Normalization Strategies for MicroRNA Quantification. Clin Chem. 2015;61(11):1333-42.

104. Schwarzenbach H. Circulating nucleic acids as biomarkers in breast cancer. Breast Cancer Res. 2013;15(5):211.

105. Chernyi VS, Tarasova PV, Kozlov VV, Saik OV, Kushlinskii NE, Gulyaeva LF. Search of MicroRNAs Regulating the Receptor Status of Breast Cancer In Silico and Experimental Confirmation of Their Expression in Tumors. Bull Exp Biol Med. 2017;163(5):655-9.

106. Tormo E, Adam-Artigues A, Ballester S, Pineda B, Zazo S, Gonzalez-Alonso P, et al. The role of miR-26a and miR-30b in HER2+ breast cancer trastuzumab resistance and regulation of the CCNE2 gene. Sci Rep. 2017;7:41309.

107. Ichikawa T, Sato F, Terasawa K, Tsuchiya S, Toi M, Tsujimoto G, et al. Trastuzumab produces therapeutic actions by upregulating miR-26a and miR-30b in breast cancer cells. PLoS One. 2012;7(2):e31422.

8. Acknowledgement

First, I would like to thank my supervisor, Ass. Prof. Dr. Heidi Schwarzenbach, for providing me the interesting research MD project, for her contributions of time, expert advices at the lab and help to write a paper, which have improved my experimental and writing experience. I also pay my thanks to the technician, Ms. Bettina Steinbach who helped me establishing the techniques.

I am deeply appreciative to Prof. Dr. Klaus Pantel, the director of the Institute of Tumor Biology, who offered me the opportunity to work at his excellent institute. I want to pay my special thanks to the secretary of the institute, Ms. Roswitha Pakusa, for her kind and valuable help in my work and study life.

I am very grateful to Prof. Dr. Volkmar Müller and Dr. Leticia Ferrer at the Department of Gynecology for their excellent collaborations. I would like to thank Dr. Eileen Waldmann, Hebke Hinz and Nicole Kunath in Cit Research Sachtleben GmbH for the helpful assistance in first part of my project covering EMF.

I also want to express my thanks to all the staff of the Institute of Tumor Biology and especially to Ines Stevic, Dr. rer. nat. Volker Aßmann and Jana Jensen for their helpfulness, technical and professional support, as well as moral encouragement.

Many thanks go to the China Scholarship Council, without the financial support, the doctoral pursuits would not be possible. Finally, I would like to thank my husband and family and all the friends who have always supported me and gave me love and strength.

9. Curriculum Vitae

Personal Information

Name: Ni, Qingtao

Date of Birth: 24/08/1990

Gender: Female

Nationality: Chinese

Email: niqingtao.seu@gmail.com

Telephone: 0162 7667 612

Educational Background

Dec, 2016: Start of MD study at University Medical Center Hamburg-Eppendorf,

Hamburg, Germany

Sep, 2014-Jul, 2016: Master of Medicine, Clinical Medicine, Infectious Diseases

Southeast University, Nanjing, Jiangsu, PR of China

Sep, 2013-Jul, 2014: Clinical internship, Nanjing First Hospital, Affiliated Nanjing Medical University, Nanjing, Jiangsu, PR of China

Sep, 2009-Jul, 2014: Bachelor of Medicine, Southeast University, Nanjing, Jiangsu,

PR of China

Awards and Honors

Scholarship from China Scholarship Council; China Scholarship Council, 2017.

Excellent intern, Southeast University, 2014

Course Award, Southeast University, 2012

Social Work Excellence Award, Southeast University, 2012

National inspirational scholarship, Southeast University, 2010

Scholarships from the Bank of China, Southeast University, 2009

Academic Experience

- Aug 2017- Jul 2018: Circulating exosomal microRNAs in blood of breast cancer patients

- Jan 2017- Jul 2017: Investigations of the effects of electromagnetic fields on breast cancer cell lines
- Apr 2015- Apr 2016: Research on thyroid hormone levels in liver failure patients
- Oct 2012- Jan 2013: Different concentrations of doxorubicin in transferred liver cancer of a mice model.
- Jun 2011: Preparation of acute liver failure model to investigate the pathogenesis of hepatic encephalopathy and its treatment.
- Mar 2011-Jul 2011: Repairment of apigenin on rabbits with acute myocardial ischemia.

Publications

1. **Ni Qingtao** et al. Different signatures of miR-16, miR-30b and miR-93 in exosomes from breast cancer and DCIS patients. (Scientific reports, submitted)

2. **Ni Qingtao** et al. Research of thyroid hormone and pituitary hormone in patients with liver failure. Chinese Hepatology. 2017; 22(8):611-616.

3. **Ni Qingtao** et al. The progress of research of thyroid hormone and pituitary hormone in patients with liver failure. Chinese Hepatology. 2016; 21(8):689-692.

4. **Ni Qingtao** et al. The prognostic model of liver failure. Chinese Journal of Practical Hepatology, 2016.19(4):500-504.

5. Pan Chi, Ines Stevic, Volkmar Müller, **Ni Qingtao** et al. Exosomal microRNAs as tumor markers in epithelial ovarian cancer. (Molecular oncology, submitted)

10. Eidesstattliche Versicherung

Ich versichere ausdrücklich, dass ich die Arbeit selbständig und ohne fremde Hilfe verfasst, andere als die von mir angegebenen Quellen und Hilfsmittel nicht benutzt und die aus den benutzten Werken wörtlich oder inhaltlich entnommenen Stellen einzeln nach Ausgabe (Auflage und Jahr des Erscheinens), Band und Seite des benutzten Werkes kenntlich gemacht habe.
Ferner versichere ich, dass ich die Dissertation bisher nicht einem Fachvertreter an einer anderen Hochschule zur Überprüfung vorgelegt oder mich anderweitig um Zulassung zur Promotion beworben habe.
Ich erkläre mich einverstanden, dass meine Dissertation vom Dekanat der Medizinischen Fakultät mit einer gängigen Software zur Erkennung von Plagiaten überprüft werden kann.

Unterschrift: Qingtao Ni